

Article

Remediation of Heavy Metals Using Biomass-Based Adsorbents: Adsorption Kinetics and Isotherm Models

Okon-Akan Omolabake Abiodun ^{1,2,3,*}, Oluwasogo Oluwaseun ⁴, Olaoye Kayode Oladayo ^{1,2},
Omoogun Abayomi ⁵, Akpowu Arubi George ⁶, Emmanuel Opatola ⁷, Robinson Friday Orah ⁸,
Efe Jeffery Isukuru ⁹, Ifunanya Chiamaka Ede ¹⁰, Oluwadara Temitayo Oluwayomi ⁸, Jude A. Okolie ¹¹
and Ibrahim Asiata Omotayo ^{3,*}

- ¹ Forestry Research Institute of Nigeria, Ibadan, Nigeria
 - ² Department of Wood and Paper Technology, Federal College of Forestry, Jericho 200284, Nigeria
 - ³ Pure and Applied Chemistry Department, Ladoko Akintola University of Technology, Ogbomosho 210214, Nigeria
 - ⁴ Soil Science Laboratory, School of Applied Biosciences, Kyungpook National University, Sangju-si 37224, Republic of Korea
 - ⁵ Department of Chemistry, University of Lagos, Lagos, Nigeria
 - ⁶ Department of Chemistry, Federal University of Agriculture, Abeokuta 111101, Nigeria
 - ⁷ Department of Materials and Metallurgical Engineering, University of Ilorin, Ilorin, Nigeria
 - ⁸ Department of Chemistry, University of Ibadan, Ibadan 200132, Nigeria
 - ⁹ Department of Environmental Management and Toxicology, Federal University of Petroleum Resources, Effurun 330102, Nigeria
 - ¹⁰ Department of Chemistry, Federal University of Technology, Minna, Nigeria
 - ¹¹ Gallogly College of Engineering, University of Oklahoma, Norman, OK 73019, USA; jude.okolie@ou.edu
- * Correspondence: okon-akan.o@frin.gov.ng (O.-A.O.A.); aoibrahim@lautech.edu.ng (I.A.O.)



Citation: Abiodun, O.-A.O.; Oluwaseun, O.; Oladayo, O.K.; Abayomi, O.; George, A.A.; Opatola, E.; Orah, R.F.; Isukuru, E.J.; Ede, I.C.; Oluwayomi, O.T.; et al. Remediation of Heavy Metals Using Biomass-Based Adsorbents: Adsorption Kinetics and Isotherm Models. *Clean Technol.* **2023**, *5*, 934–960. <https://doi.org/10.3390/cleantechnol5030047>

Academic Editor: Patricia Luis

Received: 22 February 2023

Revised: 25 March 2023

Accepted: 21 July 2023

Published: 28 July 2023

Abstract: This study aims to comprehensively investigate the current advances in water treatment technologies for the elimination of heavy metals using biomass-based adsorbents. The enhancement of adsorption capacity in biomass materials is achieved through surface modification, which increases their porosity and surface area. The study therefore focuses on the impact of different surface modification techniques on the adsorption capacity, as well as the evaluation of adsorptive removal techniques and the analysis of various isotherm and kinetics models applied to heavy metal contaminants. The utilization of kinetic and isotherm models in heavy metal sorption is crucial as it provides a theoretical background to understand and predict the removal efficiency of different adsorbent materials. In contrast to previous studies, this research examines a wide range of adsorbent materials, providing a comprehensive understanding of their efficacy in removing heavy metals from wastewater. The study also delves into the theoretical foundations of the isotherm and kinetics models, highlighting their strengths, limitations, and effectiveness in describing the performance of the adsorbents. Moreover, the study sheds light on the regenerability of adsorbents and the potential for their engineering applications. Valuable insights into the state-of-the-art methods for heavy metal wastewater cleanup and the resources required for future developments were discussed.

Keywords: adsorption; biomass; kinetic; isotherm; heavy metals; biosorption



Copyright: © 2023 by the authors. Licensee MDPI, Basel, Switzerland. This article is an open access article distributed under the terms and conditions of the Creative Commons Attribution (CC BY) license (<https://creativecommons.org/licenses/by/4.0/>).

1. Introduction

Environmental pollution has become a major threat to the ecological community due to the existence of lethal substances such as heavy metals and organic pollutants in the air, water, and soil. Rapid economic development and population growth, as well as advancement in different industries, including agriculture, is the key cause of environmental pollution [1,2]. Environmental pollutants, such as waste burning, synthetic industries, and coal conversion, pose a major danger to the abiotic environment (air, water, and soil) and biotic populations (plants, animals, and humans). Heavy metals, such as

copper, cadmium, nickel, mercury, chromium, lead, and zinc, are particularly of concern owing to their persistence in the environment. These toxic metals can get into water bodies and soil through sludge dumping and melting processes, causing serious harm to live organisms through biomagnification in food chains. Researchers have identified the elimination of dangerous metal ions from the environment as a critical issue [3–5].

Environmental toxicants often comprise dyes, pesticides, and heavy metals which cause danger to the whole ecological community, gravely compromising its function and structure [6]. The dumping of sludge and melting processes also contribute to heavy metal pollution in the environment [7]. The high levels of heavy metals in sewage sludge can cause soil pollution, which is harmful to live organisms. The health of the soil is crucial for the growth of food crops. When toxic metals are released into the soil, it severely affects the quality and output of plants, posing a serious threat to humans and animals through biomagnification in the food chain [8]. Heavy metals easily migrate from the soil to crops thereby increasing their toxicity. With large cities generating vast amounts of wastewater, it is essential to find effective ways to dispose of and handle it.

As a result, researchers have identified the full remediation of dangerous metal ions from the environment as a key issue. Over the years, various techniques have evolved to extract these ions from wastewater. These techniques include adsorption, solvent extraction, ion exchange, chemical precipitation, coagulation and flocculation, membrane processes, and oxidation [9,10]. However, these technologies have several disadvantages, including high costs and poor adsorption capability at low concentrations (1–100 mg/L) [11]. The method chosen for the restoration system is based on the properties of the wastewater, as each method has its restrictions, including efficiency, environmental impact, feasibility, cost, practicality, reliability, sludge generation, operational difficulties, preliminary treatment requirements, and the development of chemical deposits [12,13].

Adsorption is considered to be among the best strategies for eradicating pollutants, as it is simple to use, can be designed in various ways, and significantly affects biological availability, toxicity, and the transport of heavy metals in wastewater [11,14,15]. The buildup of metal ions on the surface of the sorbent occurs through a transfer process, where they are bonded chemically or physically [16,17]. All adsorption processes require a balance between solids and liquids and mass transfer rates. There are three main processes of adsorption onto solid sorbents: contaminants are transported from an unsolidified solution to the surface of the sorbent; adsorption onto a solid surface; and transit inside the sorbent particle. Heavy metals are attracted to the surface with electrostatic forces or to hydroxyl or other functional groups. The ability to desorb and regenerate adsorbents for multiple applications makes this technique highly efficient and results in well-treated effluents at a low cost. Adsorption of inorganic effluents can be used to increase water quality, preventing long-term effects on human health. Products would be pure, and valuable substances would be recovered if this were carried out.

Numerous studies have documented the adsorption of heavy metals using various biomass-based adsorbents and magnetic oxides. For example, Mostafapour et al. [18] found that immobilized *Gracilaria corticata* algae-based bioadsorbent could remove lead (II) from wastewater. Thermodynamics analyses indicated that the Pb (II) sorption on immobilized-GC was feasible, spontaneous, and endothermic, with enthalpy and entropy values of 52.01 kJ/mol and 0.185 kJ/mol K, respectively. Kinetic studies showed that the adsorption process followed the pseudo-second-order kinetic model due to the higher regression coefficient and lower error coefficient. In another study, Mahvi et al. [19] used magnetic Fe₃O₄-graphene oxide to remove chromium oxides. The removal efficiencies showed a moderate decrease in maximum values (less than 6%) after six regeneration cycles. The developed Fe₃O₄-GO composite is a promising material for removing Cr (VI) from wastewater. Sobhanikia et al. [20] demonstrated that the mucilaginous seeds of *Cydonia oblonga* can be used as an effective biosorbent for the removal of Cr particles from wastewater.

Activated carbon is a commonly used non-polar adsorbent for metal ion elimination from effluents due to its great capacity for adsorption and specific surface area. However, its high cost is a hindrance, leading researchers to explore alternatives such as agricultural waste, natural materials, and industrial byproducts for use as adsorbents. These materials are more cost effective, selective, efficient, and eco-friendly than commercial adsorbents, and are being used in wastewater treatment to remove heavy metals [21,22]. Numerous biomasses with modification, including sawdust, waste tea, coconut shell, peat moss, and rice husk are used as adsorbents [23–28]. However, studies and understanding are limited in the area of isotherm and isotherm models in heavy metal sorption.

The application of kinetic and isotherm models in heavy metal sorption is crucial as it provides a theoretical framework to understand and predict the removal efficiency of different adsorbent materials. Numerous researchers have studied the kinetics and isotherm models for biosorption of heavy metals. Agarwal et al. [29] conducted kinetic and adsorption isotherm studies on the removal of harmful nickel (II) using γ -alumina nanoparticles and multiwalled carbon nanotubes. They found that the adsorption equilibrium and kinetic data were well fitted and in good agreement with Langmuir and pseudo-second-order kinetic models, respectively. The maximum percentage removal of Ni (II) was found to be 87.65% and 99.41% using MWCNTs and γ -alumina nanoparticles, respectively, under optimum conditions. In another study, the isotherms and thermodynamic studies of Cd (II) ion removal in effluents using *Azolla filiculoides* biosorbents was documented [30]. Despite the abundance of information and studies on kinetics and isotherms, much of the data is scattered throughout the literature. Additionally, there are limited review articles available on this topic. To address the knowledge gaps, the study aims to provide information on the condition of water treatment advances today and the use of adsorptive measures with a focus on adsorption capacity and adsorption kinetics and isotherm models. The study also delves into the theoretical foundations of the isotherm and kinetics models, highlighting their strengths, limitations, and effectiveness in describing the work of the adsorbents. The research findings will be valuable for researchers, engineers, and practitioners in the areas of water treatment and environmental science as it provides an in-depth analysis of the latest advances in the use of biomass-based adsorbents for the removal of heavy metals. Moreover, the investigation also clarifies the regenerability of adsorbents and the potential for their engineering applications. The report provides valuable insights into the state-of-the-art methods for heavy metal wastewater cleanup and the resources required for future developments. In contrast to other published papers, the presented review outlines novel experimental data or new research findings relating to heavy metal removal, often focusing on specific aspects of the problem such as the development of new adsorbent materials, kinetics, and adsorption isotherms. It should be mentioned that biomass-based adsorbents are the focus of this study due to their numerous advantages. Firstly, they are cost effective and easily available, as they can be obtained from agricultural and forestry waste, algae, or other biological sources. Secondly, they are eco-friendly and renewable, making them a sustainable alternative to traditional chemical methods. Biomass-based adsorbents also have high selectivity and affinity for heavy metals, which enables them to efficiently remove these contaminants from wastewater.

2. Heavy Metals Remediation Techniques

Various approaches have been implemented to remediate heavy metals, as depicted in Figure 1. Generally, conventional technologies could be classified into physical, chemical, and biological methods. These approaches will be meticulously discussed in subsequent sections. It should be mentioned that other techniques such as sedimentation, screening, filtration, and most biological methods are outside the purview of this review. Interested readers are referred to excellent reviews by Al-Qodah et al. [31] Our previous study has also discussed the advances in nanomaterials applications for heavy metals remediation [32].

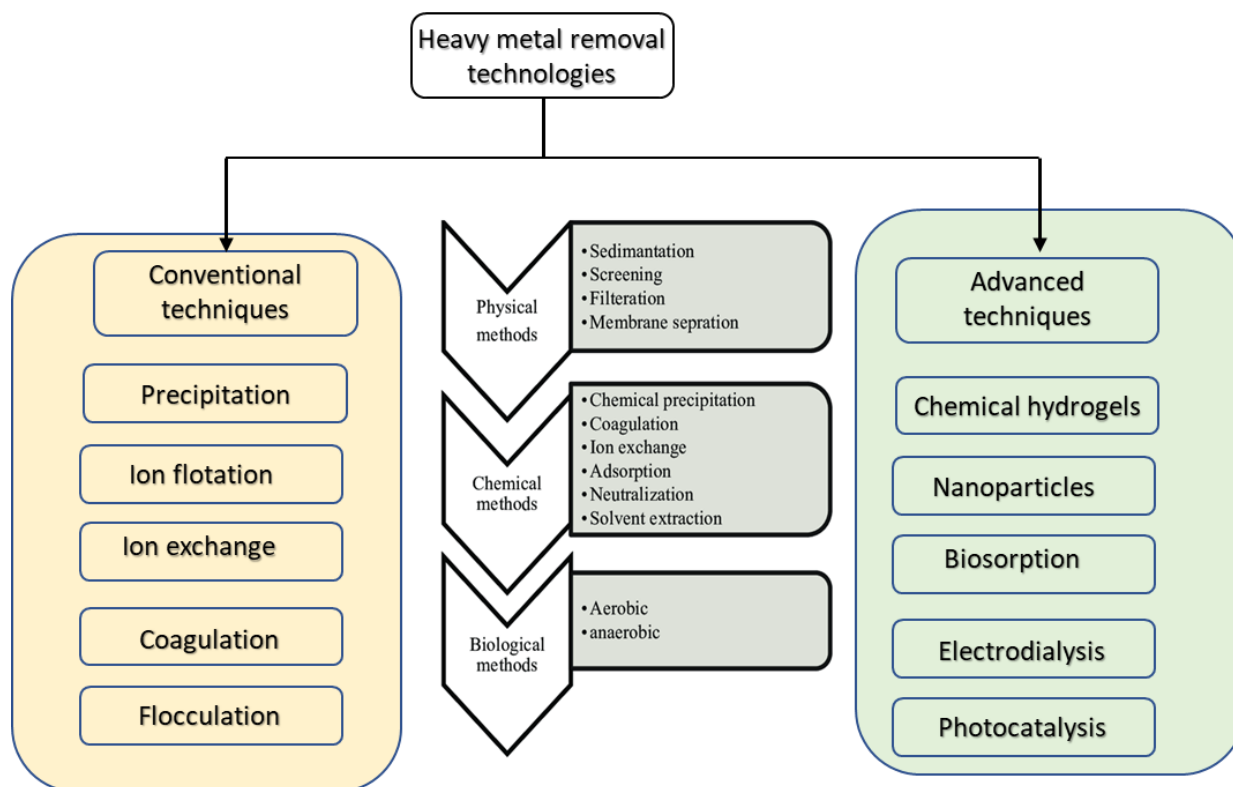


Figure 1. Common procedures for remediating metal ions from wastewater.

2.1. Chemical Precipitation

This is deployed for the removal of ionic components from wastewater by inducing a chemical process that transforms soluble material into an insoluble one. Precipitates are then removed through subsequent separation processes, such as coagulation or filtering. Hydroxide precipitation is the most frequently used approach for precipitating metals; however, sulfide and carbonate precipitation are also common [33].

Precipitation may be understood on a fundamental level by considering the following mechanism shown in reaction 1. The addition of hydroxides led to the separation of heavy metals from the waste stream, and hydroxide ion is produced.



The insoluble metal hydroxide is written as $M(OH)_2$, where M^{2+} is the metal ion, and OH^- is the precipitating agent. According to a study by Brooti et al., the efficacy of removing Fe^{3+} , Cr^{3+} , Cu^{2+} , Pb^{2+} , Ni^{2+} , and Cd^{2+} was found to be greater than 97% at an optimal $Mg(OH)_2$ dose [34]. A study by Meunier et al. showed that chemical precipitation with $Ca(OH)_2$ was efficient in decreasing Cu^{2+} , Cr^{6+} , Ni^{2+} , and Zn^{2+} in acidic soil saline leachate but not Cd^{2+} and Pb^{2+} [35]. However, chemical precipitation is ineffective for wastewater treatment with a high acid content, as it can generate a significant volume of excess sludge that requires chemical stabilization and proper disposal, which can be costly. Additionally, some metal salts are insoluble in water and require the addition of a suitable anion for precipitation. The method may not be effective for removing metal ions of low concentration and may result in high disposal costs if the sludge produced has high water content.

2.2. Coagulation and Flocculation

These are important steps in the treatment processes involved in wastewater disposal and the subsequent production of potable water. When a coagulant or chemical is added to wastewater, a chemical reaction takes place, leading to coagulation. The colloidal

components in aqueous solutions tend to cluster into larger structures called flocs. These tiny aggregates in suspension, also known as flocs, tend to attract heavier objects such as metals. When water is stirred slowly, the tiny flocs can grow and eventually descend to the solution's base. This process is called flocculation. Figure 2 illustrates these two occurrences. Coagulation and flocculation are mostly used to remove organic contaminants. A study by Alalwan et al. investigated the efficiency of ferrous sulfate heptahydrate ($\text{FeSO}_4 \cdot 7\text{H}_2\text{O}$) in reducing chemical oxygen demand (COD), total suspended solids (TSS), and biochemical oxygen demand (BOD) in palm oil mill effluent [36]. Wang et al. also conducted similar research [37]. While this process offers ease of implementation and is non-selective when it comes to separating heavy metals, it also creates a significant amount of waste and exacerbates the issue by transporting dangerous compounds into the solid phase. Despite these drawbacks, coagulation and flocculation can effectively remove unwanted substances such as dissolved metals, dyes, and suspended particles.

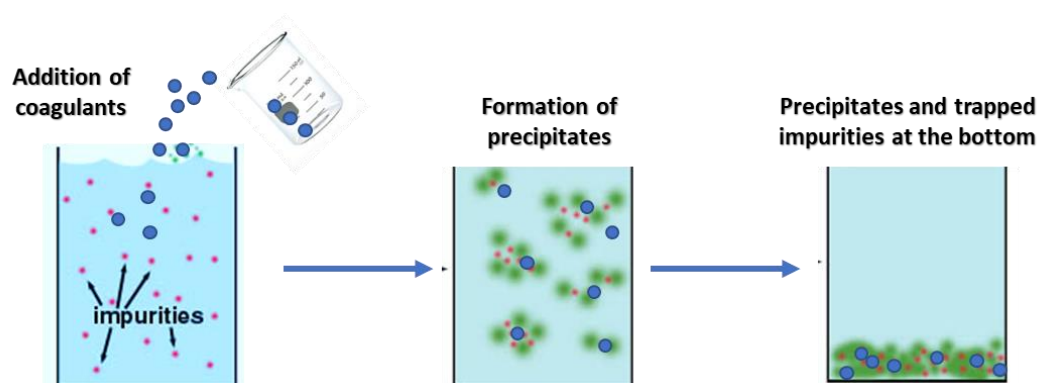


Figure 2. Schematic diagram of coagulation and flocculation methods for metal ion remediation.

2.3. Ion Flotation

This is commonly used to treat metals in wastewater from industrial processes. There are many different ways, both experimental and industrial, for purifying wastewater of metals. At a minimum airflow velocity of 1098 mL min^{-1} , 90% of Fe^{3+} and Mn^{2+} was removed from the flotation column using a biodegradable surfactant collector [38]. A synthetic surfactant, sodium oleate, was also used as a collector and was effective at removing the metals. The combination of a bio-surfactant and dissolved air flotation shows more promise than column flotation [38]. For the elimination of cadmium from water, the use of foam flotation with rhamnolipid bio-surfactant was investigated [39]. The study looked at the effects of changing the rhamnolipid and cadmium content, as well as the solution pH, aeration rate, and inertial concentration on the efficiency of separating cadmium from zinc and copper. Pseudo-first-order kinetics at a rate of 0.0071 min^{-1} showed that adipose tissue was more selective than copper and zinc, with maximum separation from zinc- and copper-contaminated solutions measured at 57% and 48%, respectively.

2.4. Electrochemical Process

This process involves a reaction of electron transfer, which can be either electro-reduction or oxidation as shown in Figure 3 [40]. Over the years, electrolytic metal recovery has garnered considerable attention. The process involves passing a direct current through a metal ion-containing solution to transport the ions from cathode plates to insoluble anodes. First, metal ions that are positively charged must make contact with the negatively charged cathode.

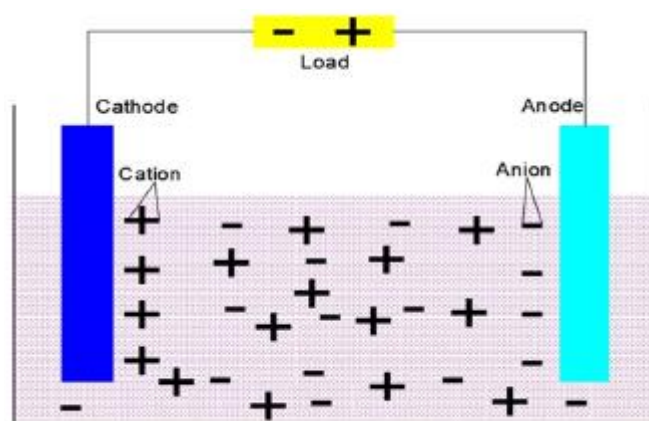


Figure 3. A schematic of the electrolytic method for heavy metals recovery.

The use of electrochemical reactors for processes such as metal recovery, electrocoagulation, electro-floatation, and electro-oxidation has a long history [41]. The efficacy of metal removal has been demonstrated to depend on the electrodes used and the cell type being utilized. Hexavalent chromium can be converted to trivalent chromium through electrochemical precipitation in an alkaline medium. Eight hours of electrolysis at pH 5.5 with 0.25 A current removes 98% of the chromium, while five hours of electrolysis at pH 1 with the same current removes 95% of the chromium. Electrochemical processes provide many benefits, such as rapid and well-controlled operation, metal selectivity, reduced sludge production, and no additional chemical demands. Because of the high cost of the electrodes and the amount of electricity needed to power the operation, this approach is limited in several ways [42].

2.5. Membrane Filtration

A study by Lee and Kwak found that membrane filtration treatment techniques performed exceptionally well in removing heavy metals from wastewater [43]. Membranes are dynamic, nanometer-scale structures that are put together to form a complex whole. Modern reverse osmosis systems typically consist of thin polymer sheets supported by a permeable support system. The membrane's ability to allow water through while rejecting heavy metal ions is largely determined by its physical and chemical characteristics [44]. The main benefits of this technology are its efficiency, small footprint, and user-friendliness. The membrane processes of nanofiltration, ultrafiltration, electrodialysis, and reverse osmosis have all been employed successfully to filter wastewater of potentially dangerous metal ions. Heavy metals are rejected by allowing water to pass through a semi-permeable membrane. This is one of the best technologies for treating water and wastewater by eliminating dissolved metals. Negative aspects of this strategy include rejection, membrane fouling, and expensive power consumption. Dissolved and colloidal solids can also be recovered using the ultrafiltration technique at low transmembrane pressure. When using an ultrafiltration membrane, the dissolved solids are generally easier to flow through because of larger pore sizes than the solids. Polymer-enhanced ultrafiltration and enhanced ultrafiltration were both successful at removing heavy metal ions [45]. Between ultrafiltration and reverse osmosis, nanofiltration serves as a transitional step. Toxic heavy metals are removed from wastewater using this treatment process [46]. Among the benefits of this treatment approach are its high efficiency, low energy consumption, dependability, and simplicity of operation [47].

2.6. Adsorption

Adsorption is a process where particles or molecules adhere to a surface, forming a thin film or layer. In the context of heavy metal removal, adsorption is a widely used method for removing heavy metal ions from wastewater. The process involves the use of adsorbents, which are materials that have a high affinity for heavy metal ions [32]. When

the wastewater is passed through a bed of adsorbent material, the heavy metal ions are adsorbed onto the surface of the adsorbent material, effectively removing them from the wastewater [48]. The extent of adsorption depends on various factors, such as the surface area of the adsorbent, the concentration of the heavy metal ions, and the pH of the solution. Adsorption is an effective method for heavy metal removal, as it can remove a wide range of heavy metals and is relatively simple to implement. However, the effectiveness of the process depends on the specific adsorbent used and the conditions under which it is used.

It is well-accepted that adsorption is the most economical, efficient, and selective approach for removing heavy metals from wastewater [49]. This method is both functionally and structurally sound, facilitating complete heavy metal remediation from wastewater. Heavy metals can be removed from wastewater by transferring them to a solid surface, or adsorbent, where they can be bound chemically or physically through adsorption across the adsorbent's surface. Adsorption can be either physical, where weak Van der Waals forces are responsible, or chemical, where a covalent bond forms between the adsorbent and adsorbate. Activated carbon (AC) is an excellent adsorbent owing to its enormous surface area and affinity for heavy metals [50]. Commercially available activated carbons can be classified as either "H" or "L" [51]. High-temperature activated carbon (H-type AC) is carbon from which the H⁺ ions have been chemically removed, while the removal of OH⁻ ions during low-temperature oxidation of carbon forms L-type AC. Incorporating specific desorption methods for heavy metals facilitates the regeneration of adsorbents that have previously absorbed these contaminants.

2.7. Innovative Technologies for the Removal of Heavy Metals from Industrial Effluent

Many innovative methods and technologies have been created to address the drawbacks of conventional methods. Some of these technologies include the use of hydrogels, multifunctional nanomaterials, and biosorption. Each of these techniques is discussed in the next section.

2.7.1. Hydrogels

Three-dimensional networks of hydrophilic polymers called hydrogels may absorb and hold a lot of water. They have a soft and gel-like texture and can swell and retain their shape when exposed to water. This property makes them useful for heavy metal remediation in wastewater. In heavy metal remediation, hydrogels act as a "sponge" in the wastewater, absorbing and retaining the metals within their structure. This helps to lower the amount of heavy metals present in the water, making it safer for discharge or reuse. The mechanism of hydrogels is mainly through ion exchange and physical entrapment.

Hydrogels are effective in the removal of a variety of heavy metals, including lead, cadmium, and zinc, from wastewater [43]. They are environmentally friendly and low-cost alternative to traditional methods. Additionally, recovery and reuse are easy since hydrogels are simply separated from the treated water. The hydrogel's most valuable attribute is its ability to retain its structural integrity despite swelling and holding enormous amounts of water. However, 10% (weight or volume) of the substance must be water-based for it to qualify as a hydrogel. Upon withdrawal of the stimulation, hydrogel often recovers to its initial state [52]. Hydrogels that are sensitive to pH, temperature, electromagnetism, and light are all examples of common hydrogel kinds. Water-soluble hydrogels can effectively remove heavy metals from various materials and have also been found useful in drug administration, tissue engineering, contact-lens technology, pH sensors, biological sensors, and biosensors [53]. Cd²⁺, Cu²⁺, and Fe³⁺ have been separated from aqueous solutions by free radical solution polymerization of Cross-linked homopolymers and copolymers of acrylamide (AM) and 2-acrylamido-2-methylpropanesulfonic acid (AMPS) [54]. When the pH of the solution is low, the hydrogel has a hard time binding metal ions. Additionally, increasing the pH of AM/AMPS hydrogels enhanced their absorption capacity. In terms of electronic configuration, ionic radius, polarity, etc., and the type of interac-

tion with hydrogel's functional groups, the order of metal ions adsorbable by hydrogel is $\text{Cd}^{2+} > \text{Cu}^{2+} > \text{Fe}^{3+}$ [55].

2.7.2. Multifunctional Nanomaterials

Multifunctional nanomaterials are materials that have multiple functions and are engineered at the nanoscale, usually with dimensions less than 100 nm. They have unique physical and chemical properties that makes them highly attractive for a wide range of applications, including heavy metal remediation in wastewater. In heavy metal remediation, multifunctional nanomaterials work by adsorbing and retaining the heavy metals in their structure, reducing the metal concentration in the wastewater. The mechanism of heavy metal adsorption by nanomaterials is mainly through ion exchange and physical entrapment, as well as through chemical interactions between the nanomaterials and heavy metals [31,32]. The mechanism can be quite complex and depend on a variety of factors, such as the type of nanomaterials, the nature of the heavy metal ion, and the conditions of the solution. Multifunctional nanomaterials demonstrate a high surface-area-to-volume ratio, allowing improved exposure to heavy metal ions in wastewater [32]. The physical and chemical interactions, including Van der Waals forces, electrostatic attraction, and hydrogen bonding, facilitate the adsorption of heavy metals onto the surface of the nanomaterials. During the ion exchange mechanism, the multifunctional nanomaterials often exchange ions with heavy metal ions in wastewater. The functional groups present on the surface of the nanomaterials can attract and bind heavy metal ions, releasing other ions in the process [31,32]. The nanomaterials can also undergo redox reactions with heavy metal ions, in which the nanomaterials donate or accept electrons from the metal ions, resulting in their removal from the wastewater.

Multifunctional nanomaterials, such as nanocomposites, nanotubes, and nanoparticles, are highly effective in removing a variety of heavy metals from wastewater, including cadmium, lead, and zinc [32]. They are environmentally friendly and low-cost alternatives to traditional methods. Additionally, these nanomaterials can be easily recovered from the treated water, facilitating regeneration of heavy metals.

The utilization of multifunctional nanomaterials, which can handle various problems more efficiently, is one of the most rapidly explored segments of wastewater treatment technology. Adsorption of magnetic nanoparticles is easier and more efficient than adsorption of other types of adsorbents in general [56]. Several metal oxide nanoadsorbents make use of their high surface areas and the functionalized groups that can be added to enhance their affinity. Zinc oxide, titanium dioxide, and cerium oxide are the three most frequent forms. Heavy metals like zinc, nickel, chrome, copper, and cadmium can be removed from water using zeolites. In Ref. [57], the study discovered a synthetic oxide based on hydrated and agglomerated nanocrystallite (11–13 nm) titanium oxide is effective at removing Ni^{2+} from water. Detailed information on different multifunctional nanomaterials for heavy metal remediation can be found elsewhere [31].

2.7.3. Biosorption

Biosorption has developed as a viable and environmentally benign alternative for the removal of heavy metals from wastewater effluent generated by some enterprises. Biosorption is a physiochemical process in which metal ions are bonded to the surface of a biosorbent. Biopolymers and precursors from both agricultural and industrial waste streams are among the many potential metal sorbents. For the removal of trace amounts of heavy metals and their subsequent recovery, biosorption is regarded as an important technology. *Chlorella vulgaris*, enriched activated sludge, and nitrifier-enriched activated sludge were used in varied ratios to test nutrient removal, carbon capture, and metabolite synthesis (NAS) [58]. In biosorption, the biological materials act as a “sponge” for the heavy metals in the wastewater, absorbing and retaining the metals within their structure [59,60]. This helps to reduce the concentration of heavy metals in the water, making it safer for discharge or reuse. The mechanism of heavy metal adsorption by biosorbents is mainly through

ion exchange, physical entrapment, and chemical interactions between the biosorbent and heavy metal ions.

Biosorbents produced from biomass have low mechanical strength as they are unstable, susceptible to degradation, and very prone to a change in the arrangement of the molecules of the biosorbents. Easily degradable also means that they may not be reusable as adsorption capacity is likely to reduce after initial use [61]. It is also usually hard to regain all the metals accumulated on the surface of the biosorbents by adsorption since biosorbents are scattered in the mixture. Finally, the biosorbents cannot be used again because they wear down under harsh circumstances, and their ability to adsorb greatly reduces.

Because of the challenges listed above, it is necessary to fix biosorbents to the right surface before using them in traditional unit systems like packed/fluidized bed reactors and continuously stirred tank reactors, that way ensuring optimum uptake capacity and reuse over several cycles. This is known as the immobilization of biomass. There are different techniques used for the immobilization of biomass. They include the following:

1. **Entrapment:** This technique is relatively cheap and uses reagents such as polyurethane, polysulfone, and so on. However, there is mass transfer resistance [62].
2. **Crosslinking:** This technique provides increased strength. The disadvantages are that there is a loss of activity, and it is not universal. Examples of reagents are formaldehyde and nitro [62].
3. **Encapsulation:** This technique prevents biosorbents leakage and had higher catalyst densities. However, it produces fragile capsules and mass transfer resistance. It makes use of reagents such as cellulose, gelatine, and polyvinyl acetate [63].
4. **Adsorption:** This technique is cheap and simple and encourages higher biomass loading. However, there are risks of unstable binding and possible leakage of biosorbents. Examples of biosorbents include active charcoal, carbon nanotubes, and ceramics [64–68]. Table 1 shows the advantages and limitation of several heavy metal remediation techniques.

Table 1. The advantages and limitations of the presented heavy metal remediation methods. Adapted from Refs. [31,64–68].

Heavy Metal Remediation Methods	Advantages	Limitations
Activated carbon promoted adsorption	High efficiency	Expensive, regeneration challenges
Modified biopolymer promoted biosorption	Improved adsorption capacity and selectivity	Difficulties in the optimization of operating conditions and the selection of the most promising bio-sorbent
Coagulation and precipitation	Ease of operating	High chemical consumption Costly process, sludge disposal issues in the case of precipitation
Electrochemical methods	High removal capacity and selectivity Does not require a chemical	High capital and operating cost
Ion exchange	High selectivity for metal ions and ease of regeneration	Expensive process
Membrane filtration	High metal separation selectivity, requires low space	High operating cost in most cases
Nanofiltration	Could simultaneously remove metals and organic pollutants	Long-duration and restricted applications

3. Heavy Metal Removal Using Biomass-Based Adsorbent

Heavy metal removal using biomass-based adsorbent is an environmentally friendly approach to remediate contaminated water. Biomass materials like agricultural waste, food waste, and algae are utilized to create adsorbent materials that can effectively remove toxic heavy metals like lead, mercury, and cadmium. This method is cost effective, renewable, and sustainable compared to traditional chemical methods. Agricultural residues have a

free and pore structure, which contains carboxyl and hydroxyl that contribute to adsorption processes such as a diversity of agricultural solid wastes, like coconut, tealeaf, wheat barn, rice shell, sawdust obtained from a walnut shell, cotton stalks, coffee beans, banana peels, groundnut shells, sugar beet pulp, sugarcane bagasse, cassia fistula leaves, and others [69]. It makes use of waste and the utilization of garbage, which contributes to the solution of unusable material and environmental problems.

Common biomass adsorbent materials include soy protein, nutshells, potato peels, algae, and waste from tea [70]. Due to the great metal selectivity of biomass, it can be made available again without causing much waste to recover more metal, which creates less sludge and is more efficient [71]. Because these biomass materials do not require extensive and costly preparation, they are a viable alternative to conventional adsorbents which are characterized as unrenovable adsorbents.

Adsorbents made from biomass are effective and promising at removing pollutants like heavy metals and dyes and other contaminants from wastewater. Biomass, being a collection of constituents, possesses a varied range of characteristics. The components of biomass adsorbent materials that are non-toxic and environmentally benign include cellulose, lignin, and chitin [69,72]. Sugarcane pulp is mostly constituted of carbohydrates such as lignin (20–25%), cellulose (40–50%), and polyose (25–30%). In [73], the authors reported that the majority of the rice husk is composed of moisture (10–15%), cellulose (50%), silica (15–20%), and lignin (25–30%). The hull of rice contributes to around 20% of the grain's weight. Rice husk has a bulk density of between 90 and 150 kg per cubic meter.

3.1. Overview of Agricultural Waste Adsorbent (AWB)

AWBs have been used in various studies to completely replace traditional techniques of heavy metal cleaning due to their significant advantages. For this reason, AWBs have a far higher affinity for heavy metals than other adsorbents, due to their surface's plethora of binding groups [74]. Due to the numerous components of agricultural origin used in AWBs, their cost is often low [75]. It is also environmentally friendly because AWBs may be processed, applied, and retrieved without causing any damage [47]. These AWB characteristics were crucial in industrial applications, making AWBs a better adsorbent choice [76]. However, adsorption capacity is not the only thing to consider when selecting an AWB. There are just a few biosorbents that can be used in the process of large-scale biosorption and that have an irrevocable space and selectivity for heavy metals. Researchers believe that for an air–water barrier to be effective, it must meet several requirements, including the ability to be widely available and inexpensive while also having high regeneration and low release rates of unexpected components in an aqueous solution [76].

An excellent adsorbent material is rice husk because of the low cost and long-term sustainability of this resource. The chemical compositions of rice husks are as follows: cellulose content of 32%, a hemicellulose content of 20%, a lignin content of 21%, and the remaining organic components, such as protein and fat, account for the remaining 20%. To further pollute the environment, rice husks are commonly thrown into the soil or burned. However, rice husks can be transformed into value-added products via thermochemical processes, e.g., combustion pyrolysis and gasification. It has been found that the removal of inorganic components through the surface of rice husk (such as silica and carbonate) enhance adsorption capacities. In addition, the ash produced by rice husk might be as high as 20%. Because of the large surface area and its high porosity, ash production contains over 95% of silica and skeleton maintenance of the cellular structure. Contact time and temperature affect the ash's porosity and functional groups, hence resulting in a diversity of ash varieties. During combustion, the cellulose–lignin core burns away, revealing a porous silica skeleton that is ground into extremely small particles with a large surface area.

There are various advantages to using sawdust as an adsorbent for heavy metal adsorption, making it a fascinating material to investigate. Waste from sawmills and its low price make sawdust a common commodity [77]. Because sawdust is biodegradable, it should harm neither the environment nor any of its constituents if it is disposed of in

this manner. Research into the adsorption mechanism of sawdust is possible because of its structure and contents. The sawdust's structure and components make it a research topic in the field of adsorption at 30 °C and 60 °C [78].

Adsorbent–Adsorbate Interaction

During the process of adsorption, the surfaces of the adsorbent and adsorbate interact before reaching equilibrium. Adsorption of an adsorbate onto an adsorbent primarily involves three key mechanisms: physical adsorption, precipitation and complexation, and pore-filling [79]. The adsorption can be broken down into three distinct stages: the clear zone (initial phase), the mass transfer zone (intermediate phase), and the exhausted or saturated zone (final phase) where equilibrium is achieved. The clear and saturated zones demonstrate an inverse relationship. Except for a rise in the concentration of the adsorbate, the mass transfer zone remains relatively unchanged until the breakthrough point when the adsorbent becomes fully saturated [80]. Organic molecules tend to bind to the adsorbent through van der Waals forces, hydrophobic interactions, and hydrogen bonds. Conversely, adsorption of metals (inorganic compounds) primarily occurs through processes such as ion exchange, surface electrostatic attraction, and precipitation.

Different types of biochars exhibit unique mechanisms for heavy metal adsorption, greatly influenced by their surface properties. The existence of surface functional groups on biochars, especially oxygen-containing groups like carboxylates and hydroxyls, enhances the interaction strength between the biochar surface and heavy metals. This interaction alters the surface functional groups of the biochars both before and after inorganic contaminant adsorption [81]. Other factors like surface area, pore structure, and mineral constituents of biochar also significantly contribute to the adsorption of inorganic contaminants [82].

The present study acknowledges a research gap in understanding the effects of nanoconfinement on the process of heavy metal adsorptive removal. Nanoconfinement can shift the interactions between heavy metals and adsorbent from a general electrostatic attraction to a specific innersphere coordination. This shift indicates a significant increase in adsorption selectivity towards these contaminants, with promising adsorption distribution coefficients.

4. Adsorption Kinetics Models

In the past, several models and mathematical equations have been employed to explain the mechanisms [83] and adsorption kinetics [79,84] of adsorption processes. Specifically, the capacity of different solutes for equilibrium adsorption. The chemical and physical characteristics of adsorbents influence the adsorption mechanism as well. These models are reviewed in the next section. Also, the following assumptions are inherent in these models:

- Equilibrium conditions: Many isotherm models assume that the biosorption process reaches equilibrium, meaning that the amount of heavy metal adsorbed onto the adsorbent no longer changes with time.
- Homogeneous adsorption surface: Many isotherm models assume that the adsorption surface of the biosorbent is homogeneous, meaning that all active sites on the adsorbent have the same properties.
- First-order reaction kinetics: Some kinetic models assume that the adsorption process follows first-order reaction kinetics, meaning that the rate of adsorption is directly proportional to the concentration of the heavy metal.
- Pseudo-second-order kinetics: Other kinetic models assume that the adsorption process follows pseudo-second-order kinetics, meaning that the rate of adsorption is proportional to the square of the concentration of the heavy metal.
- Langmuir isotherm: The Langmuir isotherm model assumes that the adsorption occurs on a homogeneous surface with a fixed number of active sites that have the same adsorption energy.

- Freundlich isotherm: The Freundlich isotherm model assumes that the adsorption occurs on a heterogeneous surface, meaning that the active sites have different adsorption energies.
- BET isotherm: The BET isotherm model assumes that the adsorbent surface consists of multiple layers of adsorption sites, and that the adsorption energy decreases with increasing coverage of the surface.

It should be mentioned that these assumptions are implemented to help in the simplification and mathematical computations of the models. While they do not always present an accurate representation of the model complexities, their influence in ease of computing the model is significant. Extreme caution should be taken during the implementation of these assumptions.

4.1. Pseudo-First Order Lagergren Model

It is usual to utilize the pseudo-first order (PFO) kinetic model to describe how boundary diffusion affects adsorption. It is the adsorption model that is most usually employed. To explain the kinetics of liquid–solid phase adsorption, Lagergren provided a first-order rate equation. For solute adsorption from liquid, the pseudo-first order kinetic model is frequently utilized [85–89]. It is claimed to be the original adsorption capacity model [90]. It is used to illustrate how different species’ adsorption kinetics work. The PFO model developed by Lagergren is remarkably suited for lower solute concentrations [86]. Over the years, it has been widely utilized to explain the adsorption of toxins and pollutants from wastewater in a variety of fields. In some areas, it has recently gained popularity as a way to explain the sorption of pollutants from wastewater. It can be presented as shown in Equations (1) and (2) in Table 2.

Table 2. Critical evaluation of different adsorption kinetic models together with their underlying equations.

Type	Expression	Equation	Ref.
Lagergren pseudo-first order	$\log(Q_e - Q_t) = \log Q_e - \frac{k_1 t}{2.303}$	(2)	[91–93]
	$\ln(Q_e - Q_t) = \ln Q_e - k_1 t$	(3)	[94]
Pseudo-second order	$\frac{t}{Q_t} = \frac{1}{Q_e} t + \frac{1}{k_2 \cdot Q_e^2}$	(4)	[90,95]
Intraparticle diffusion model	$Q_t = k_1 t^{1/2} + I$	(5)	[96–99]
Avrami	$Q_t = Q_{av} \left(1 - e^{-(k_{av} t)^{n_{av}}} \right)$ $\ln(-\ln(1 - Q_t)) = \ln(K_{av}) - n_{av} \ln(t)$	(6)	[89,90]
Bangham	$Q_t = Q_e - (Q_e - Q_0) \exp(-k_b t^m)$	(7)	[100]
	$\log\left(\log \frac{C_t}{C_i} - Q_t m\right) = \log K_0 - Q_t \log(t)$	(8)	[15]
Boyd	$B_t = -0.4977 - \ln\left(1 - \frac{Q_t}{Q_e}\right)$	(9)	[15]
Elovich	$Q_t = \frac{1}{\beta} \ln(\alpha\beta) - \frac{1}{\beta} \ln(t)$	(10)	[101]

Q_e refers to the adsorption capacity at equilibrium, measured in mg/g. Q_t represents the adsorption capacity at a specific time point t , also expressed in mg/g. The constant k_1 denotes the pseudo-first-order adsorption equilibrium rate constant, measured in 1/min, while t stands for the time of contact in minutes. The constant k_2 represents the equilibrium rate constant of pseudo-second-order adsorption, measured in $g \cdot mg^{-1} \cdot min^{-1}$. The intra-particle diffusion rate constant is represented by k_i , measured in $mg \cdot g^{-1} \cdot min^{-0.5}$, while I is a constant that provides information about the thickness of the boundary layer, expressed in $mg \cdot g^{-1}$. The term $t_{1/2}$ stands for half-life time. Q_{av} signifies the Avrami theoretical value of the quantity of adsorption, measured in $mg \cdot g^{-1}$, while K_{av} is the Avrami constant rate, and n_{av} is the Avrami order model. Q_t also signifies the quantity of adsorbate in the adsorbent at a certain time point t , expressed in $mg \cdot g^{-1}$. C_t refers to the solution concentration at time t , whereas C_i stands for the initial concentration of the adsorbate, measured in $mg \cdot L^{-1}$. Again, Q_t refers to the quantity of adsorbate in the adsorbent at time t , quantified in $mg \cdot g^{-1}$. m refers to the mass of the adsorbent in a liter of adsorbate, measured in $g \cdot L^{-1}$. k_b is the rate constant for Bangham’s model. B_t stands for the Boyd constant. β represents the number of available sites for adsorption, while α stands for the initial adsorption rate, measured in $mg \cdot g^{-1} \cdot min$.

4.2. Lagergren Pseudo Second-Order-Model

The adsorption mechanism, equilibrium adsorption capacity, and rate constants of adsorption processes can be calculated using the Lagergren pseudo second-order (PSO) model technique [87]. It can be presented as shown in Equation (3) in Table 2.

4.3. Intraparticle Diffusion Model

The intraparticle diffusion model is a popular approach used to examine the adsorption of heavy metals in wastewater. This model is based on the assumption that the adsorption process proceeds in three phases: external mass transfer, intraparticle diffusion, and equilibrium. During the intraparticle diffusion phase, heavy metal ions permeate into the adsorbent particles and attach to the active sites on their surface. Several factors can influence this diffusion process, including the concentration gradient, the adsorbent material's pore size, and the boundary layer's thickness.

Typically, the speed of intraparticle diffusion is slower than that of external mass transfer, making it a potential rate-limiting step in the adsorption process. The intraparticle diffusion model provides valuable insights into the mechanics of heavy metal adsorption and can help optimize the design of adsorption systems for wastewater treatment. Understanding the dynamics of the adsorption process allows researchers and engineers to devise more efficient and cost-effective methods for heavy metal removal from wastewater.

This model was developed to determine if the rate-limiting step in an adsorption process is intraparticle diffusion [88]. It posits that membrane diffusion can be overlooked, with intraparticle diffusion (IPD) being the sole phase that influences the rate [84]. Additionally, Doan et al. affirmed that the IPD stage often serves as the rate-limiting step in adsorption processes [96]. This is expressed as Equation (4) in Table 2.

4.4. The Avrami Kinetic Model

Adsorption kinetics in this model is an exponential function of adsorption time. It was developed to analyze crystal growth and phase transition in materials. When applying the Avrami model, it is important to take the mole fraction of the gas phase and the temperature of sorption into account [89,90]. The Avrami model can be applied when there are several adsorption mechanisms and depends on the overall rate of adsorption. It is presented as shown in Equation (5) in Table 2.

4.5. The Bangham Kinetic Model

The rate-controlling stage of an adsorption process has also been identified using the Bangham kinetic model. The equation can also be expressed as shown in Equations (6) and (7).

4.6. The Boyd Kinetic Model

This model distinguishes between intraparticle diffusion and extra-particle diffusion and can be mathematically expressed as shown in Equation (8).

4.7. Elovich Kinetic Model

Lately, the kinetics of gas adsorption on solids as well as the adsorption of pollutants from aqueous solutions have both been described by the Elovich equation on several occasions. The underlying premise of Elovich's model is that solid surfaces are actively diverse. It is described mathematically in Table 2 as Equation (9).

5. Adsorption Isotherm Models

Different isotherm models have been utilized to evaluate the response performance amongst pollutants and the adsorbent of interest for heavy metal remediation [102–105]. Table 3 compiles the mathematical formulas for frequently employed isotherms. The special attributes and features that these isotherms may be further applied to were also supplied.

Table 3. Mathematical expression in both non-linear and linear forms for frequently used isotherms.

Isotherm	Non-Linear Form	Eq.	Linear Form	Eq.	Plot	Ref.
Langmuir	$Q_e = \frac{K_L Q_L C_e}{1 + K_L C_e}$	(11)	$\frac{C_e}{Q_e} = \frac{1}{K_L Q_L} + \frac{C_e}{Q_L}$	(12)	$\frac{C_e}{Q_e}$ vs. C_e	[106]
			$\frac{1}{Q_e} = \frac{1}{K_L Q_L C_e} + \frac{1}{Q_L}$	(13)	$\frac{1}{Q_e}$ vs. $\frac{1}{C_e}$	
			$Q_e = Q_L - \frac{Q_e}{C_e K_L}$	(14)	Q_e vs. $\frac{Q_e}{C_e K_L}$	
			$\frac{Q_e}{C_e} = K_L (Q_L - Q_e)$	(15)	$\frac{Q_e}{C_e}$ vs. Q_e	
Freundlich	$Q_e = K_F C_e^{1/n}$	(16)	$\frac{Ln(Q_e)}{Ln(K_F) + \frac{1}{n} Ln(C_e)}$	(17)	$Ln(Q_e)$ vs. $Ln(C_e)$	[107]
Bohart–Adams	$\frac{C_t}{C_i} = \frac{e^{K_{BA} C_i t}}{e^{K_{BA} N_0 \frac{Z}{U} - 1} + e^{-K_{BA} C_i t}}$	(18)	$\frac{Ln(\frac{C_t}{C_i} - 1) = \frac{K_{BA} N Z}{U} - K_{BA} C_i t$	(19)	–	[108]
Brunauer–Emmett–Teller (BET)	$\frac{Q_e}{(C_s - C_e)(1 + (C_{BET} - 1)(\frac{C_e}{C_s}))} = \frac{Q_s C_{BET} C_e}{(C_s - C_e)(1 + (C_{BET} - 1)(\frac{C_e}{C_s}))}$	(20)	$\frac{C_e}{Q_e(C_s - C_e)} = \frac{1}{Q_s C_{BET}} + \frac{(C_{BET} - 1)(\frac{C_e}{C_s})}{Q_s C_{BET}}$	(21)	$\frac{C_e}{Q_e(C_s - C_e)}$ vs. $\frac{C_e}{C_s}$	[109]
Dubinin–Radushkevich	$Q_e = Q_{DR} e^{-\beta \epsilon^2}$	(22)	$Ln(Q_e) = Ln(K_{DR} \epsilon^2)$	(23)	$Ln(Q_e)$ vs. ϵ^2	[110]
Flory–Huggins	$\frac{\theta}{C_i} = K_{FH} (1 - \theta)^{n_{FH}}$	(24)	$\log(\frac{\theta}{C_i}) = \log(K_{FH}) + n_{FH} \log(1 - \theta)$	(25)	$\log(\frac{\theta}{C_i})$ vs. $\log(1 - \theta)$	[111]
Frenkel–Halsey–Hill	$\ln(\frac{C_e}{Q_e}) = \frac{-\alpha}{RT} (\frac{Q_s}{Q_e d})^r$	(26)	–	–	–	[112]
Khan	$Q_e = \frac{Q_s b_k C_e}{(1 + b_k C_e) a_k}$	(27)	–	–	–	[113]
Koble–Corrigan	$Q_e = \frac{A(C_e)^n}{1 + B(C_e)^n}$	(28)	$\frac{1}{Q_e} = \frac{1}{A(C_e)^n} + \frac{B}{A}$	(29)	–	[114]
MacMillan–Teller	$Q_e = Q_s (\frac{k}{Ln \frac{C_e}{C_s}})^{\frac{1}{3}}$	(30)	–	–	–	[115]
Radke–Prausnitz	$Q_e = \frac{a_{RP} r_R (C_e)^{\beta_R}}{a_{RP} + r_R (C_e)^{\beta_R - 1}}$	(31)	–	–	–	[116]
Redlich–Peterson	$Q_e = \frac{K_R C_e}{1 + a_R C_e^g}$	(32)	$\ln(K_R \frac{C_e}{C_s} - 1) = g \ln C_e - \ln a_R$	(33)	–	[117]
Sips	$Q_e = \frac{K_s C_e^{\beta_s}}{1 + a_s C_e^{\beta_s}}$	(34)	$\beta_s \ln C_e = -\ln \frac{K_s}{Q_e} + \ln a_s$	(35)	$\ln \frac{K_s}{Q_e}$ vs. $\ln C_e$	[118]
Temkin	$Q_e = \frac{RT}{b_T} \ln A_T C_e$	(36)	$Q_e = \frac{RT}{b_T} \ln A_T + \frac{RT}{b_T} \ln C_e$	(37)	Q_e vs. $\ln C_e$	[119]
Toth	$Q_e = \frac{K_T C_e}{(a_T + C_e)^{\frac{1}{T}}}$	(38)	$\ln(\frac{Q_e}{K_T}) = \ln C_e - \frac{1}{T} \ln(a_T + C_e)$	(39)	$\ln(\frac{Q_e}{K_T})$ vs. $\ln C_e$	[120]
Wolborska	$\frac{C_t}{C_i} = e^{(\frac{\beta C_i}{N_0} t - \frac{\beta Z}{U})}$	(40)	–	–	–	[121]
Yoon–Nelson	$\frac{C_t}{C_i} = \frac{1}{1 + e^{-K_{YN}(t - \tau)}}$	(41)	–	–	–	[122]
Harkins–Jura	–	–	$\frac{1}{Q_e^2} = \frac{B_{HJ}}{A_{HJ}} - \frac{1}{A_{HJ}} \log C_e$	(42)	$\frac{1}{Q_e^2}$ vs. $\log C_e$	[123]
Halsey	–	–	$\frac{Ln(Q_e)}{\frac{1}{n_H} Ln(K_H) - \frac{1}{n_H} Ln(C_e)}$	(43)	$Ln(Q_e)$ vs. $Ln(C_e)$	[123]
Elovich–Larionov	–	–	$\frac{Ln Q_e}{Ln(K_E Q_E) - \frac{1}{Q_E} Q_e}$	(44)	$n \frac{Q_e}{C_e}$ vs. Q_e	[124]

Q_L (Langmuir isotherm monolayer adsorption)—this is the maximum adsorption capacity, reflecting the maximum amount of adsorbate that can be adsorbed in forming a monolayer on the surface; K_L (Langmuir constant)—this relates to the affinity of the binding sites and the energy of adsorption; C_e is the equilibrium concentration of the adsorbate; Q_e is the amount of adsorbate per unit weight of adsorbent at equilibrium; K_F is the Freundlich isotherm constant (mg/g) (L/g)ⁿ—this relates to adsorption capacity; n : adsorption intensity; K_{BA} (Bohart–Adams constant)—this is a rate constant used in the Bohart–Adams model to describe adsorption kinetics in a column system; Z is the total depth of the bed containing the adsorbent; C_{BET} (Brunauer–Emmett–Teller) isotherm model—this relates to the energy of the surface interaction; C_s is the saturation concentration for a monolayer of

adsorbate; Q_s is theoretical isotherm saturation capacity (mg/g); K_{DR} is the Dubinin–Radushkevich isotherm constant (mol^2/k^2); Q_{DR} is the theoretical isotherm saturation capacity (mg/g); C_i is the adsorbate initial concentration (mg/L); K_{FH} is the Flory–Huggins isotherm equilibrium constant (L/g); n_{FH} is the Flory–Huggins isotherm model exponent; θ is the degree of surface coverage; d is the interlayer spacing (m); R is the universal gas constant (8.314 J/mol/K); r is the inverse power of distance from the surface; T is temperature (K); α is the Frenkel–Halsey–Hill isotherm constant ($\text{J m}^r/\text{mole}$); a_k is the Khan isotherm model exponent; b_k is the Khan isotherm model constant; A is the Koble–Corrigan isotherm constant ($\text{L}^n \cdot \text{mg}^{1-n} \cdot \text{g}^{-1}$); B is the Koble–Corrigan isotherm constant (L/mg) ^{n} ; n : adsorption intensity; a_{Rp} is the Radke–Prausnitz isotherm model constant; r_R is the Radke–Prausnitz isotherm model constant; β_R is the Radke–Prausnitz isotherm model exponent. a_R is the Redlich–Peterson isotherm constant (L/mg); g is the Redlich–Peterson isotherm exponent; K_R is the Redlich–Peterson isotherm constant (L/g); a_s is the Sips isotherm model constant (L/mg); K_s is the Sips isotherm model constant (L/g); β_s is the Sips isotherm model exponent; A_T is the Temkin isotherm equilibrium binding constant (L/g); b_T is the Temkin isotherm constant; a_T is the Toth isotherm constant (L/mg); K_T is the Toth isotherm constant (mg/g); t is the Toth isotherm constant; C_t is the solution concentration at the fixed bed outlet at time t ; N_0 is the maximum volumetric sorption capacity; U is the linear flow rate; Z is the total bed depth; β is the kinetic coefficient of the external mass transfer; K_{YN} is the Yoon–Nelson rate constant; τ is the time required for reaching 50% adsorbate breakthrough (min); A_{HJ} is the Harkins–Jura isotherm constants (slope); B_{HJ} is the Harkins–Jura isotherm constants (intercept); K_H is the Halsey Constant (slope); n_H is the Halsey Constant (intercept); K_E is the Elovich–Larionov isotherm constant; Q_E is the Elovich–Larionov maximum adsorption capacity (mg/g).

Langmuir’s isotherm model adopts the fact that a single layer is formed when there is biosorption without some form of relationship amongst the molecules adsorbed on the adsorbent. According to Zhou et al. [125], the Langmuir isotherm in its non-linear form is written as seen in Equation (1), while its linear models are expressed in Equations (12)–(15). Scientists used this model often to study environmental adsorption because of its ease of usage [126,127] based on the structure and surface of solids. Another commonly used model is the Freundlich isotherm, which assumes the biosorption process happens on different pores of the adsorbent and that the concentration of adsorbates is related to sorption capacity [128]. The non-linear is expressed in Equation (16), while the linear model is represented in Equation (17). Temkin’s isotherm assumes the heat of sorption globules is comparative to adsorbent dosage. It has a factor that shows in a clear way how the adsorbed particles are linked to the adsorbent. It is written as a non-linear equation (Equation (36)) and a linear equation (Equation (37)).

Most of the time, the Dubinin–Radushkevich (DR) model accounts for the porous structure effect of adsorbent and it assumes adsorption depends on micropore volume fillings; it can be expressed in non-linear (Equation (22)) and linear (Equation (23)) form. When adsorption is performed via column or fixed bed, the Bohart–Adams isotherm is used. When Bohart and Adams developed their model in 1920, its reliance on surface reaction theory and the assumption that equilibrium is not instantaneous are what give it its distinctiveness. The Bohart–Adams model’s performance can be assessed using the non-linear (Equation (18)) and linear (Equation (19)) equations [129–131]. The BET isotherm was developed to bridge the gap in the Langmuir model by extending between successive layers, according to the Langmuir theory of multilayer adsorption and dynamic equilibrium [132,133]. This model is expressed in non-linear (Equation (20)) and linear (Equation (21)) form. The Flory–Huggins solution theory, which is used to describe the coverage properties of an adsorbate, holds that the chain elements organize themselves arbitrarily on a three-dimensional structure [134]. This isotherm is expressed in non-linear (Equation (24)) and linear (Equation (25)) form [135–139].

The Frenkel–Halsey–Hill isotherm principle believes that a metal atom only uses pair potentials to interact with other types (adsorbate and substrate) and assumes the interface between the adsorbent and metal ions does not connect adsorbate molecules through three-body interaction terms [140]. The expression of this isotherm is in non-linear form (Equation (26)) [141,142]. The Khan theory was developed for multi-component and single adsorption frameworks and synthesized Langmuir and Freundlich’s limitations [142], and Equation (27) [121] provides a non-linear expression for this isotherm. The Koble–Corrigan

isotherm employs the Langmuir and Freundlich isotherms principle as a three-parameter equation to determine the equilibrium of diverse systems. Ref. [143] used the model to simulate a surface with different types of adsorption sites [144,145]. This model can be expressed mathematically as a non-linear (Equation (28)) and linear (Equation (29)) equation. Ref. [146] say that the Hill and Koble–Corrigan models have the same mean relative percent error. This shows that these models are similar and are set up in the same way [147,148]. In the Brunauer–Emmett–Teller isotherm, surface tension effects have been added to the MacMillan–Teller isothermal model [149]. A non-linear model can be used to express this isotherm (Equation (30)).

Radke–Prausnitz isotherm, which is written as a non-linear equation, recognizes that an adsorbent should be thermodynamically inactive [144]. For instance, its features, such as internal energy, have no bearing on the adsorption process (Equation (31)). Because it is so adaptable and works in both homogeneous and heterogeneous systems, the Redlich–Peterson model is used [150]. Both a non-linear equation (Equation (32)) and a linear equation can be used to represent this isotherm (Equation (33)) [142,151]. The Sips scientific model works well if the adsorption is limited and the adsorbates do not interact with each other [152,153]. It is expressed as a non-linear equation (Equation (34)) and linear equation (Equation (35)). Langmuir’s model is the basis for Toth’s model, which was developed to describe heterogeneous adsorption systems in both low and high concentrations. It is expressed as a non-linear equation (Equation (38)) and a linear equation (Equation (39)) [154,155]. The Wolborska model looks at adsorption kinetics utilizing the mass exchange conditions relating to the diffusion means at low levels [156]. It is expressed as a non-linear equation (Equation (40)) [130,157].

The Yoon–Nelson model assumes that the adsorbate particle’s chance of adsorption is decreasing at a faster rate than the adsorbent is moving forward [153]. A non-linear equation is used to represent it (Equation (41)) [130,158]. The Harkins–Jura isotherm considers the possibility of multilayer adsorption on the surface of the adsorbent having a heterogeneous pore distribution [159]. Mathematically, this model can be expressed as a linear equation (Equation (42)) [147]. Ref. [160] assumed Halsey’s isothermal model is mostly about the multilayer adsorption mechanism [147]. It is expressed as a linear equation (Equation (43)). The non-electrolyte adsorption of a solution onto a solid surface is depicted by the Elovich–Larionov isotherm. The formula is a linear equation (Equation (44)). An overview of different research studies showing the selected biomass adsorbent’s adsorption kinetics and isotherm models for removing heavy metals is presented in Table 4.

Table 4. Adsorption kinetics and isotherm models of selected biomass adsorbent for heavy metal removal.

S/N	Materials	Heavy Metal	Initial Conc.	Adsorbent Dose	pH	Temperature	Adsorption Capacity/Removal Efficiency	Kinetics	Isotherms	Mechanisms
1	Red seaweed <i>Kappaphycus</i> sp.	Pb ²⁺ Cu ²⁺ Fe ²⁺ Zn ²⁺	10 mg/L.	4 g	2–7	25	22.27 19.46 17.09 16.78 mg/g	IPD	Temkin model	xxx
2	Sunflower-based adsorbent	Cd ²⁺ Cu ²⁺ Cr ⁶⁺ Ni ²⁺	50 mg/L	4 g	2		3.2 mg/g– 252.5 mg/g	PSO	Langmuir	xxx
3	L-cysteine (Cys) intercalated MgAl-layered double hydroxide (MgAl-Cys-LDH)	Cu ²⁺ Pb ²⁺ Cd ²⁺	100 mg/L 300 mg/L 100 mg/L	0.05 g	5.0 5.73 5.85	25	58.07 186.2 93.11 mg/g	PSO	Langmuir	xxx

Table 4. Cont.

S/N	Materials	Heavy Metal	Initial Conc.	Adsorbent Dose	pH	Temperature	Adsorption Capacity/Removal Efficiency	Kinetics	Isotherms	Mechanisms
4	Recycling spent lithium-ion battery: spent lithium iron phosphate (SLFP) spent lithium manganate (SLMO) cathodes	Cu ²⁺ Pb ²⁺ Cd ²⁺ Zn ²⁺	100 mg/L	0.5 g	6 5 6 6	25	44.28, 39.54, 25.63, and 27.34 mg/g and 32.51, 31.83, 26.24 and 25.25 mg/g	PSO	Langmuir	xxx
5	Bamboo stem biomass	Pb ²⁺ Cd ²⁺	50 mg/L	0.25–2 g	5	25	95.92 80.98%	PSO	Freundlich	xxx
6	EDTA-modified agricultural by-product-based adsorbent: ethylenediaminetetraacetic acid-modified lotus seedpod (EDTA-LSP)	Pb ²⁺ malachite green (MG).	100 mg/L	5 mg	5 6	25	225.88 mg/g 347.87 mg/g	PSO	Langmuir	xxx
7	Biochar of date palm waste	Pb ²⁺ Cu ²⁺	50–250 mg/L	1.0 g 1.8 g	4.5 5.5	30	98.9 mg/g 41 mg/g	PSO	Freundlich-Langmuir and H-J isotherms	xxx
8	Graphene	NO ³⁻	500 mg/L	0.05 g	7	30	89.97 mg/g	PSO	Langmuir	xxx
9	Fe ₃ O ₄ /montmorillonite nanocomposite (Fe ₃ O ₄ /MMTNC)	Pb ²⁺ Cu ²⁺ Ni ²⁺	510.16 182.94 111.90 mg/L	0.06 g 0.08 g 0.08 g	Same as the solution pH	25	89.72%, 94.89%, and 76.15%	PSO	Langmuir	electrostatic attraction and coordination
10	Activated carbons (ACs) from chickpea (Cicer arietinum) husks	Pb ²⁺ Cr ²⁺ Cu ²⁺	100–400 mg/L	2–6 g	2–10	20–40	135.8 59.6 56.2 mg/g	PSO	Freundlich	xxx
11	Microwave-functionalized cellulose derived from rice husk	Pb ²⁺ Cd ²⁺ Ni ²⁺	10–300 mg/L.	1–4 g	2–8 2–7 2–5.5	20, 35, 50	295.20 mg/g 151.51 mg/g 72.80 mg/g	PSO	Langmuir	ion exchange and chelation, physical adsorption
12	Self-activation of kenaf fiber and then the kenaf-based activated carbon (KAC)	lead Pb ²⁺ copper Cu ²⁺ Congo red (CR) dye	5 mg/L	1.5 g/L	4–7	27	92% 80% 95%	PSO	Langmuir (for Cu ²⁺) and Freundlich models (for Pb ²⁺ and CR)	physical adsorption and chemical adsorption
13	Mixed biomass [Aspergillus campestris and two forms of Delonix regia seed (raw and acid-treated Delonix regia seed)]	Cu ²⁺	10 to 100 mg/L	1.0 g	6	30	62.02 mg/g and 66.9 mg/g	PSO	Freundlich isotherm model	physical adsorption (physisorption) mechanism

Table 4. Cont.

S/N	Materials	Heavy Metal	Initial Conc.	Adsorbent Dose	pH	Temperature	Adsorption Capacity/Removal Efficiency	Kinetics	Isotherms	Mechanisms
14	Thiol-functionalized mesoporous silica-coated magnetite nanoparticles	Ni ²⁺ Cu ²⁺ Cr ³⁺	2 mg/L 2 mg/L 8 mg/L	0.008 to 0.04 g	7 10 10	25	4.476, 4.038, and 1.119 mg/g	PSO, PSO, and PFO	Langmuir Langmuir Freundlich	
15	Cross-linked chitosan-g-acrylonitrile copolymer	Cr ⁶⁺ Cu ²⁺ Ni ²⁺	200 mg/L	6 g 6 g 5 g	5 5 5.5	30	84% 86% 81%	PSO	Freundlich isotherm model	xxx
16	Iminodiacetic acid functionalized D301 resin	Cu ²⁺ Pb ²⁺ Cd ²⁺	10 mg/L	0.01 g	5	20	4.48 2.99 2.26 mg/g	PFO	Langmuir	chemisorption
17	Beech sawdust	Cu ²⁺ Ni ²⁺ Zn ²⁺	0.2 mg/L	1 g	4.8–5.3	25	4.5 mg/g 4 mg/g 2 mg/g	PSO	Langmuir	ion exchange mechanism
18	Treated old newspaper	Cd ²⁺	30 mg/L	0.33–1 g	6.4	22	8.41 mg/g 2.87 mg/g	PSO	Langmuir	xxx
19	Sugarcane Bagasse (SCB)	Hg ²⁺	76 mg/L	1–7 g	4	30	35.71 mg/g	PSO	Freundlich and Langmuir models	xxx
20	Grapefruit peel	Cd ²⁺ Ni ²⁺	50 mg/L	4 g	5	20–50	42.09 46.13 mg/g	PSO	Freundlich isotherm model	ion exchange mechanism
21	Peanut shell biomass	Cu ²⁺ Cr ³⁺	100 mg/L	10 g	5	20	25.39 mg/g 27.86 mg/g	PSO	Langmuir	physical sorption
22	Zeolite Based on Oil Shale Ash	Cu ²⁺ Ni ²⁺ Pb ²⁺ Cd ²⁺	500 mg/L	0.05 g	6 6 5 5	20–50	224.72 156.74 118.34 53.02 mg/g	PSO	Langmuir	ion exchange mechanism
23	Untreated coffee grounds	Cd ²⁺	100 mg/L	9 g	7	20	15.65 mg/g	PSO	Langmuir	electrostatic interaction
24	Cellulosic waste orange peel (CWOP)	Cu ²⁺	100 mg/L	1 g	5	20–50	63 mg/g	external mass transfer kinetic model	Freundlich adsorption isotherm model	xxx
25	Thiacalix [4]arene-loaded resin	Cu ²⁺ Pb ²⁺ Cd ²⁺	25 to 125 mg/L	0.1 g	2–7	10–40	21.4 47.9 44.9 mg/g	PSO	Langmuir model	xxx
26	Hierarchical CaCO ₃ -maltose meso/macroporous hybrid materials	Pb ²⁺ Cd ²⁺ Cu ²⁺ Co ²⁺ Mn ²⁺ Ni ²⁺	300–900 mg/L	0.43 g	7	25	3242.48 487.80 628.93 393.70 558.66 769.23 mg/g	PSO and IPD	Langmuir model	precipitation
27	Ethyl acrylate grafted chitosan	Pb ²⁺ Cd ²⁺ Zn ²⁺	100 mg/L	0.15 g	6	25	92% 86% 98%	PSO	Langmuir model	physical

Table 4. Cont.

S/N	Materials	Heavy Metal	Initial Conc.	Adsorbent Dose	pH	Temperature	Adsorption Capacity/Removal Efficiency	Kinetics	Isotherms	Mechanisms
28	Novel Fe ₃ O ₄ magnetic nanoparticles (MNPs) modified with 3 aminopropyltriethoxysilane (APS) and copolymers of acrylic acid (AA) and crotonic acid (CA)	Cd ²⁺ Zn ²⁺ Pb ²⁺ Cu ²⁺	20–450 mg/L	0.05 g	5.5	25	29.6 43.4 166.1 126.9 mg/g	PSO	Langmuir model	chemisorption
29	<i>Eriobotrya japonica</i> seed biocomposite	Cu ²⁺	75 mg/L	0.1 g	5	45	46.94 mg/g	PSO	Langmuir model	chemisorption
30	Native Groundnut husk	Cu ²⁺	10 to 200 mg/L	0.8 g	6	25	15.36 mg/g	PSO	Langmuir model	ion exchange
31	Bencylhexadecyl dimethyl ammonium chloride, BCDMACl	Cu ²⁺ Zn ²⁺	50–200 mg/L	0.5 g	5–6	25	50.76 mg/g 35.21 mg/g	PSO	Langmuir model	cation exchange and replacement
32	Nitrogen-doped magnetic carbon nanoparticles	Cr ³⁺	12.82 mg/L	0.01 g	8	25	12.28 mg/g	PSO	Langmuir model	ion exchange
33	Novel eco-friendly synthesized Alginate-Au nanoparticles-Mica bionanocomposite	Pb ²⁺ Cu ²⁺	50 mg/L	0.01 g	4 6 6	35	224.97 169.817 177.745 mg/g	PSO	Freundlich Langmuir Freundlich	dissociative adsorption mechanism
34	Natural Moroccan Clay	Cd ²⁺	10–200 mg/L	0.8 g	5	25–55	5.25 mg/g	PSO	Langmuir model	chemisorption
35	Shanghai silty clay	Cd ²⁺ Pb ²⁺ As ⁵⁺ Cr ⁶⁺	100 mg/L 100 mg/L 50 mg/L 50 mg/L	4 to 40 g 4 to 40 g 10 to 60 g 10 to 60 g	7	25	26.46 8.90 2.80 1.85 mg/g	PSO	Langmuir Langmuir Freundlich Freundlich	Chemical precipitation ion exchange complexation
36	Xanthate watermelon rind	As ⁵⁺ As ³⁺	4 mg/L	1 g	8.2	20	96% 98%	PSO	Langmuir isotherm	
37	Watermelon rind in a well-stirred batch system	Cu ²⁺ Zn ²⁺ Pb ²⁺	10 mg/L	0.5 g	5.0 6.8 6.8	20	6.281 mg/g 6.845 mg/g 98.063 mg/g	PSO	Langmuir adsorption isotherm	ion exchange and micro-precipitation
38	Dried potato peel (DPP)	Cu ²⁺	25–300 mg/L	0.25–1.5 g	2–5	25	84.74 mg/g	PSO	Langmuir and Freundlich models	
39	Husk powder (PHP),	Pb ²⁺ Mn ²⁺ Cd ²⁺ Ni ²⁺ Co ²⁺	20 mg/L	5 g	6	25 ± 2 °C	100% 41% 45% 24% 30%		Langmuir	
40	Green algae specie (<i>Spirogyra</i> and <i>Cladophora</i> spp)	Cu ²⁺ Pb ²⁺	100 mg/L	1.0 g	5	25	92.5–85.1%, 88.0%, and 82.6%		Langmuir Freundlich model	physical adsorption and chemical adsorption

xxx means not detected.

6. Reusability of Biomass-Based Adsorbent

Biomass-based adsorbents have demonstrated promising results for the removal of heavy metals from wastewater, but their real-time application on a large scale is still challenging. One of the major limitations is the low adsorption capacity of biomass materials, which can be addressed by surface modification techniques such as physical or chemical activation, impregnation, or coating. However, these modifications are time-consuming and require substantial resources, making it difficult to apply them on a large scale. Additionally, the regeneration of spent adsorbents is another critical factor that affects the real-time application of biomass-based adsorbents. Nonetheless, recent advances in the design and synthesis of novel adsorbents have shown potential for large-scale applications, such as the development of magnetic nanocomposites or functionalized nanomaterials. Further research is needed to optimize these adsorbent materials and to develop efficient and cost-effective regeneration methods, which will enable their practical implementation on a large scale.

Researchers are interested in the regeneration of adsorbents through desorption. Adsorbents are stabilized by the use of this procedure, which also lowers the need for virgin materials, makes it easier to recover adsorbate, and provides insight into whether an adsorption process is reversible [83,84,88]. Used biosorbents are stirred with particular chemicals under particular pH, temperature, and time conditions to achieve desorption.

In order to regenerate modified biochar, acids, primarily HNO_3 or HCl , are typically used. As a result of their struggle for active sites, the hydronium ions from these acids are released into an aqueous solution and displace metals. Thus, metal ions are removed from the adsorbents' surface [48]. As an alternative, alkalis like NaOH or NH_4OH have been utilized in an aqueous solution to lessen the protonation of modified biochar's surface, leading to the desorption of metal ions [161]. Wu et al. [161] recently showed how MnO_2 -modified biochar may be regenerated from deionized water using 0.3 M HNO_3 and 0.5 M NaOH . Their findings showed that even after five cycles of reuse, the initial adsorption capacity when the virgin-modified biosorbents were utilized was 92% for Cd ions and 80% for Pb ions, respectively. This removal capacity was greater than 15 mg/g and 34 mg/g for both Cd and Pb ions, respectively. Moreover, the Wu et al. study completed five cycles of Cd and Pb desorption from Mg-coated biochar using 1.0 M NaOH , and their findings showed q_{max} values of 92 mg/g and 272 mg/g for Cd and Pb following regeneration. Furthermore, complexing agents with electron-rich donating groups, including ethylene diamine tetraacetic acid (EDTA), have found use in the regeneration of biosorbents [162].

Hence, a regeneration study can help us better understand how biosorbents are recycled. When the raw ingredients for biosorbents are in short supply, or the synthesis is expensive and time-consuming, this helps to lower the demand for raw materials.

7. Conclusions, Challenges and Perspectives

In order to remove heavy metals, the use of modified adsorbents with biomass-based origins has increased during the last few decades based on the ability of modifying agents to improve the surface qualities of biomass materials for efficient adsorption. To evaluate the effectiveness of their adsorption, several operational parameters, isotherms, kinetics, and computational methods have been employed. The use is now restricted to laboratory-scale operations, making their expansion to commercial/large-scale production necessary. New methods and technologies should also be thoroughly investigated in order to balance the effectiveness of adsorbents with associated manufacturing costs.

However, the global production of large amounts of agricultural waste without conversion to sustainable goods has been blamed for rural pollution and, to some extent, increased difficulty in producing rural agriculture. As a result, the development of sustainable goods made from agricultural wastes effectively lowers the level of air pollution caused by agricultural waste incineration. Concerning climate change, water treatment, and general environmental protection, the development of adsorbents made from biomass has been suggested to play an important role. In addition, according to reports from all

over the world, the improvement in biomass-based adsorbents' adsorption capabilities has attracted a lot of attention and support. This has sparked a search for agents that can be added to biomass-based adsorbents to increase their adsorption capacity even more.

On the other hand, the intricacy of the modification process, its cost ramifications, and the environmental problems connected to diverse chemical modifying agents have all received significant attention. The most widely competitive green and sustainable technological strategy is said to be the exploitation of agricultural wastes to produce bio-carbon. Currently, this is concentrating on emission reduction, climate change mitigation, resource cycle, energy saving, and environmental waste management. As a result, the following perspective should be used to assess the future of biomass-based adsorbents:

- (1) It is important to develop and improve a technique for carbonizing agricultural waste to encourage the commercialization of biomass-based adsorbents.
- (2) The advancement of extremely effective green modifying substances and processes for use in the biological sorption process is also necessary.
- (3) Possible future investigations should be expanded to incorporate the use of biomass-based adsorbents to address engineering problems on a pollution scale.

Conclusively, agricultural wastes have advantages over biomass-based adsorbents and can be utilized to replace expensive commercial activated carbon in environmental protection applications.

Author Contributions: O.-A.O.A.: Conceptualization, investigation, methodology, data curation, validation, visualization, writing-original draft preparation, and writing- review, and editing. O.O., O.K.O., O.A., A.A.G., E.O., R.F.O., E.J.I., I.C.E. and O.T.O.: data curation, visualization, writing-original draft preparation. J.A.O. and I.A.O.: Contributed to material, data curation, validation, and supervision. All authors read and approved the manuscript.

Funding: This research received no external funding.

Institutional Review Board Statement: Not applicable.

Informed Consent Statement: Not applicable.

Data Availability Statement: Not applicable.

Conflicts of Interest: The authors declare no conflict of interest.

References

1. Omoarukhe, F.O.; Epelle, E.I.; Ogbaga, C.C.; Okolie, J.A. Stochastic Economic Evaluation of Different Production Pathways for Renewable Propylene Glycol Production via Catalytic Hydrogenolysis of Glycerol. *React. Chem. Eng.* **2022**, *8*, 184–198. [[CrossRef](#)]
2. Ali, M.M.; Ali, M.L.; Islam, M.S.; Rahman, M.Z. Preliminary Assessment of Heavy Metals in Water and Sediment of Karnaphuli River, Bangladesh. *Environ. Nanotechnol. Monit. Manag.* **2016**, *5*, 27–35. [[CrossRef](#)]
3. Choudhry, A.; Sharma, A.; Khan, T.A.; Chaudhry, S.A. Flax Seeds Based Magnetic Hybrid Nanocomposite: An Advance and Sustainable Material for Water Cleansing. *J. Water Process. Eng.* **2021**, *42*, 102150. [[CrossRef](#)]
4. Huang, L.; Cheng, J.; Zhang, H.; Wang, Z.; Benettayeb, A.; Seihoub, F.Z.; Pal, P.; Ghosh, S.; Usman, M.; Chia, C.H.; et al. Chitosan Nanoparticles as Potential Nano-Sorbent for Removal of Toxic Environmental Pollutants. *Nanomaterials* **2023**, *13*, 447. [[CrossRef](#)]
5. Benettayeb, A.; Ghosh, S.; Usman, M.; Seihoub, F.Z.; Sohoo, I.; Chia, C.H.; Sillanpää, M. Some Well-Known Alginate and Chitosan Modifications Used in Adsorption: A Review. *Water* **2022**, *14*, 1353. [[CrossRef](#)]
6. Nibali, L.; Buti, J.; Barbato, L.; Cairo, F.; Graziani, F.; Jepsen, S. Adjunctive Effect of Systemic Antibiotics in Regenerative/Reconstructive Periodontal Surgery—A Systematic Review with Meta-Analysis. *Antibiotics* **2022**, *11*, 8. [[CrossRef](#)]
7. Ouyang, D.; Zhuo, Y.; Hu, L.; Zeng, Q.; Hu, Y.; He, Z. Research on the Adsorption Behavior of Heavy Metal Ions by Porous Material Prepared with Silicate Tailings. *Minerals* **2019**, *9*, 291. [[CrossRef](#)]
8. Kumar, P.S.; Gayathri, R.; Rathi, B.S. A Review on Adsorptive Separation of Toxic Metals from Aquatic System Using Biochar Produced from Agro-Waste. *Chemosphere* **2021**, *285*, 131438. [[CrossRef](#)]
9. Jiang, L.; Liu, Y.; Zeng, G.; Liu, S.; Que, W.; Li, J.; Li, M.; Wen, J. Adsorption of 17 β -Estradiol by Graphene Oxide: Effect of Heteroaggregation with Inorganic Nanoparticles. *Chem. Eng. J.* **2018**, *343*, 371–378. [[CrossRef](#)]
10. Ahsan, M.A.; Islam, M.T.; Hernandez, C.; Castro, E.; Katla, S.K.; Kim, H.; Lin, Y.; Curry, M.L.; Gardea-Torresdey, J.; Noveron, J.C. Biomass Conversion of Saw Dust to a Functionalized Carbonaceous Materials for the Removal of Tetracycline, Sulfamethoxazole and Bisphenol A from Water. *J. Environ. Chem. Eng.* **2018**, *6*, 4329–4338. [[CrossRef](#)]

11. Salleh, M.A.M.; Mahmoud, D.K.; Karim, W.A.W.A.; Idris, A. Cationic and Anionic Dye Adsorption by Agricultural Solid Wastes: A Comprehensive Review. *Desalination* **2011**, *280*, 1–13. [CrossRef]
12. Liu, X.; Steele, J.C.; Meng, X.Z. Usage, Residue, and Human Health Risk of Antibiotics in Chinese Aquaculture: A Review. *Environ. Pollut.* **2017**, *223*, 161–169. [CrossRef] [PubMed]
13. Yahya, M.A.; Al-Qodah, Z.; Ngah, C.W.Z. Agricultural Bio-Waste Materials as Potential Sustainable Precursors Used for Activated Carbon Production: A Review. *Renew. Sustain. Energy Rev.* **2015**, *46*, 218–235. [CrossRef]
14. Yousafzai, A.M.; Ullah, F.; Bari, F.; Raziq, S.; Riaz, M.; Khan, K.; Nishan, U.; Sthanadar, I.A.; Shaheen, B.; Shaheen, M.; et al. Bioaccumulation of Some Heavy Metals: Analysis and Comparison of *Cyprinus Carpio* and *Labeo Rohita* from Sardaryab, Khyber Pakhtunkhwa. *BioMed Res. Int.* **2017**, *2017*, 1–5. [CrossRef] [PubMed]
15. Benjelloun, M.; Miyah, Y.; Akdemir Evrendilek, G.; Zerrouq, F.; Lairini, S. Recent Advances in Adsorption Kinetic Models: Their Application to Dye Types. *Arab. J. Chem.* **2021**, *14*, 103031. [CrossRef]
16. Kumar, A.; Gupta, H. Activated Carbon from Sawdust for Naphthalene Removal from Contaminated Water. *Environ. Technol. Innov.* **2020**, *20*, 101080. [CrossRef]
17. Gupta, G.K.; Mondal, M.K. Mechanism of Cr(VI) Uptake onto Sagwan Sawdust Derived Biochar and Statistical Optimization via Response Surface Methodology. *Biomass Convers. Biorefin.* **2020**, *13*, 709–725. [CrossRef]
18. Mostafapour, F.K.; Mahvi, A.H.; Khatibi, A.D.; Saloot, M.K.; Mohammadzadeh, N.; Balarak, D. Adsorption of Lead(II) Using Bioadsorbent Prepared from Immobilized *Gracilaria Corticata* Algae: Thermodynamics, Kinetics and Isotherm Analysis. *Desalination Water Treat.* **2022**, *265*, 103–113. [CrossRef]
19. Mahvi, A.H.; Balarak, D.; Bazrafshan, E. Remarkable Reusability of Magnetic Fe₃O₄-Graphene Oxide Composite: A Highly Effective Adsorbent for Cr(VI) Ions. *Int. J. Environ. Anal. Chem.* **2021**, *103*, 1910250. [CrossRef]
20. Bazrafshan, E.; Sobhanikia, M.; Mostafapour, F.K.; Kamani, H.; Balarak, D. Global Nest Chromium Biosorption from Aqueous Environments by Mucilaginous Seeds of *Cydonia Oblonga*: Kinetic and Thermodynamic Studies. *Glob. Nest J.* **2017**, *19*, 269–277.
21. Crini, G. Recent Developments in Polysaccharide-Based Materials Used as Adsorbents in Wastewater Treatment. *Prog. Polym. Sci.* **2005**, *30*, 38–70. [CrossRef]
22. Zhang, C.; Wang, W.; Duan, A.; Zeng, G.; Huang, D.; Lai, C.; Tan, X.; Cheng, M.; Wang, R.; Zhou, C.; et al. Adsorption Behavior of Engineered Carbons and Carbon Nanomaterials for Metal Endocrine Disruptors: Experiments and Theoretical Calculation. *Chemosphere* **2019**, *222*, 184–194. [CrossRef] [PubMed]
23. Bello, O.S.; Moshood, M.A.; Ewetumo, B.A.; Afolabi, I.C. Ibuprofen Removal Using Coconut Husk Activated Biomass. *Chem. Data Collect.* **2020**, *29*, 100533. [CrossRef]
24. Pehlivan, E.; Altun, T.; Cetin, S.; Iqbal Bhangar, M. Lead Sorption by Waste Biomass of Hazelnut and Almond Shell. *J. Hazard. Mater.* **2009**, *167*, 1203–1208. [CrossRef]
25. Jiao, G.J.; Ma, J.; Li, Y.; Jin, D.; Ali, Z.; Zhou, J.; Sun, R. Recent Advances and Challenges on Removal and Recycling of Phosphate from Wastewater Using Biomass-Derived Adsorbents. *Chemosphere* **2021**, *278*, 130377. [CrossRef]
26. Sher, F.; Iqbal, S.Z.; Albazzaz, S.; Ali, U.; Mortari, D.A.; Rashid, T. Development of Biomass Derived Highly Porous Fast Adsorbents for Post-Combustion CO₂ Capture. *Fuel* **2020**, *282*, 118506. [CrossRef]
27. Natarajan, S.; Lee, Y.S.; Aravindan, V. Biomass-Derived Carbon Materials as Prospective Electrodes for High-Energy Lithium- and Sodium-Ion Capacitors. *Chem. Asian J.* **2019**, *14*, 936–951. [CrossRef]
28. Liu, Z.; Zhang, F.S. Removal of Lead from Water Using Biochars Prepared from Hydrothermal Liquefaction of Biomass. *J. Hazard. Mater.* **2009**, *167*, 933–939. [CrossRef]
29. Agarwal, S.; Tyagi, I.; Gupta, V.K.; Dehghani, M.H.; Jaafari, J.; Balarak, D.; Asif, M. Rapid Removal of Noxious Nickel (II) Using Novel γ -Alumina Nanoparticles and Multiwalled Carbon Nanotubes: Kinetic and Isotherm Studies. *J. Mol. Liq.* **2016**, *224*, 618–623. [CrossRef]
30. Balarak, D. A Joghataei Isotherms and Thermodynamics of CD (II) Ion Removal. *Int. J. Pharm.* **2016**, *8*, 15780–15788.
31. Al-Qodah, Z.; Yahya, M.A.; Al-Shannag, M. On the Performance of Bioadsorption Processes for Heavy Metal Ions Removal by Low-Cost Agricultural and Natural by-Products Bioadsorbent: A Review. *Desalination Water Treat.* **2017**, *85*, 339–357. [CrossRef]
32. Epelle, E.I.; Okoye, P.U.; Roddy, S.; Gunes, B.; Okolie, J.A. Advances in the Applications of Nanomaterials for Wastewater Treatment. *Environments* **2022**, *9*, 141. [CrossRef]
33. Vareda, J.P.; Valente, A.J.; Durães, L. Assessment of Heavy Metal Pollution from Anthropogenic Activities and Remediation Strategies: A Review—ScienceDirect. Available online: <https://www.sciencedirect.com/science/article/pii/S0301479719307546> (accessed on 23 May 2022).
34. Brbooti, M.M.; Abid, B.A.; Al-shuwaiki, N.M. Removal of Heavy Metals Using Chemicals Precipitation. *Eng. Technol. J.* **2011**, *29*, 595–612.
35. Meunier, N.; Drogui, P.; Montané, C.; Hausler, R.; Blais, J.-F.; Mercier, G. Heavy Metals Removal from Acidic and Saline Soil Leachate Using Either Electrochemical Coagulation or Chemical Precipitation. *J. Environ. Eng.* **2006**, *132*, 545–554. [CrossRef]
36. Alalwan, H.A.; Kadhom, M.A.; Alminshid, A.H. Removal of Heavy Metals from Wastewater Using Agricultural Byproducts. *J. Water Supply Res. Technol. AQUA* **2020**, *69*, 99–112. [CrossRef]
37. Wang, L.K.; Hung, Y.T.; Shammass, N.K. *Physicochemical Treatment Processes*; Humana Press: Totowa, NJ, USA, 2005; ISBN 1588291650.

38. Albuquerque, C.F.; Luna-Finkler, C.L.; Rufino, R.D.; Luna, J.M.; De Menezes, C.T.B.; Santos, V.A.; Sarubbo, L.A. Evaluation of Biosurfactants for Removal of Heavy Metal Ions from Aqueous Effluent Using Flotation Techniques. *Int. Rev. Chem. Eng.* **2012**, *4*, 156–161.
39. Gao, G.; Xie, S.; Zheng, S.; Xu, Y.; Sun, Y. Two-Step Modification (Sodium Dodecylbenzene Sulfonate Composites Acid-Base) of Sepiolite (SDBS/ABsep) and Its Performance for Remediation of Cd Contaminated Water and Soil. *J. Hazard. Mater.* **2022**, *433*, 128760. [CrossRef]
40. Tran, H.N.; Wang, Y.F.; You, S.J.; Chao, H.P. Insights into the Mechanism of Cationic Dye Adsorption on Activated Charcoal: The Importance of π - π Interactions. *Process Saf. Environ. Prot.* **2017**, *107*, 168–180. [CrossRef]
41. Du, X.; Hao, X.; Wang, Z.; Guan, G. Electroactive Ion Exchange Materials: Current Status in Synthesis, Applications and Future Prospects. *J. Mater. Chem. A* **2016**, *4*, 6236–6258. [CrossRef]
42. Raouf MS, A.; Raheim ARM, A. Removal of Heavy Metals from Industrial Waste Water by Biomass-Based Materials: A Review. *J. Pollut. Eff. Control.* **2016**, *5*, 1–13. [CrossRef]
43. Lee, J.H.; Kwak, S.Y. Rapid Adsorption of Bisphenol A from Wastewater by β -Cyclodextrin-Functionalized Mesoporous Magnetic Clusters. *Appl. Surf. Sci.* **2019**, *467–468*, 178–184. [CrossRef]
44. Azimi, A.; Azari, A.; Rezakazemi, M.; Ansarpour, M. Removal of Heavy Metals from Industrial Wastewaters: A Review. *ChemBioEng Rev.* **2017**, *4*, 37–59. [CrossRef]
45. Xu, D.; Huang, Y.; Jin, X.; Sun, T. Synergistic Treatment of Heavy Metals in Municipal Solid Waste Incineration Fly Ash with Geopolymer and Chemical Stabilizers. *Process. Saf. Environ. Prot.* **2022**, *160*, 763–774. [CrossRef]
46. Ariffin, N.; Mustafa, M.; Bakri, A.; Remy, M.; Mohd, R.; Zaino, A.; Murshed, M.F.; Faris, M.A. Review on Adsorption of Heavy Metal in Wastewater by Using Geopolymer. *MATEC Web Conf.* **2017**, *97*, 1–8. [CrossRef]
47. Wan Ngah, W.S.; Hanafiah, M.A.K.M. Removal of Heavy Metal Ions from Wastewater by Chemically Modified Plant Wastes as Adsorbents: A Review. *Bioresour. Technol.* **2008**, *99*, 3935–3948. [CrossRef]
48. Mukherjee, A.; Okolie, J.A.; Niu, C.; Dalai, A.K. Techno—Economic Analysis of Activated Carbon Production from Spent Coffee Grounds: Comparative Evaluation of Different Production Routes. *Energy Convers. Manag.* **2022**, *14*, 100218. [CrossRef]
49. Joseph, L.; Jun, B.M.; Flora, J.R.V.; Park, C.M.; Yoon, Y. Removal of Heavy Metals from Water Sources in the Developing World Using Low-Cost Materials: A Review. Available online: <https://www.sciencedirect.com/science/article/abs/pii/S0045653519308616> (accessed on 30 September 2021).
50. Kaveeshwar, A.R.; Kumar, P.S.; Revellame, E.D.; Gang, D.D.; Zappi, M.E.; Subramaniam, R. Adsorption Properties and Mechanism of Barium (II) and Strontium (II) Removal from Fracking Wastewater Using Pecan Shell Based Activated Carbon. *J. Clean. Prod.* **2018**, *193*, 1–13. [CrossRef]
51. Chen, J.; Feng, J.; Yan, W. Facile Synthesis of a Polythiophene/TiO₂ Particle Composite in Aqueous Medium and Its Adsorption Performance for Pb(II). *RSC Adv.* **2015**, *5*, 86945–86953. [CrossRef]
52. Jasmani, L.; Rusli, R.; Khadiran, T.; Jalil, R.; Adnan, S. Application of Nanotechnology in Wood-Based Products Industry: A Review. *Nanoscale Res. Lett.* **2020**, *15*, 207. [CrossRef]
53. Joshi, M.K.; Lee, S.; Tiwari, A.P.; Maharjan, B.; Poudel, S.B.; Park, C.H.; Kim, C.S. Integrated Design and Fabrication Strategies for Biomechanically and Biologically Functional PLA/ β -TCP Nanofiber Reinforced GelMA Scaffold for Tissue Engineering Applications. *Int. J. Biol. Macromol.* **2020**, *164*, 976–985. [CrossRef]
54. Yang, Z.; Peng, H.; Wang, W.; Liu, T. Crystallization Behavior of Poly(ϵ -Caprolactone)/Layered Double Hydroxide Nanocomposites. *J. Appl. Polym. Sci.* **2010**, *116*, 2658–2667. [CrossRef]
55. Gad, Y.H. Preparation and Characterization of Poly(2-Acrylamido-2-Methylpropane-Sulfonic Acid)/Chitosan Hydrogel Using Gamma Irradiation and Its Application in Wastewater Treatment. *Radiat. Phys. Chem.* **2008**, *77*, 1101–1107. [CrossRef]
56. Okon-Akan, O.A.; Olaoye, K.O.; Ibrahim, A.O. Characterization of Activated Carbon Produced from Teak (*Tectona grandis*) Sawdust. *Sci. J. Field Wood Eng.* **2022**, *18*, 21–25.
57. Debnath, S.; Ghosh, U.C. Nanostructured Hydrous Titanium(IV) Oxide: Synthesis, Characterization and Ni(II) Adsorption Behavior. *Chem. Eng. J.* **2009**, *152*, 480–491. [CrossRef]
58. Sepehri, A.; Sarrafzadeh, M.H.; Avateffazeli, M. Interaction between *Chlorella Vulgaris* and Nitrifying-Enriched Activated Sludge in the Treatment of Wastewater with Low C/N Ratio. *J. Clean. Prod.* **2020**, *247*, 119164. [CrossRef]
59. Benettayeb, A.; Haddou, B. New Biosorbents Based on the Seeds, Leaves and Husks Powder of *Moringa Oleifera* for the Effective Removal of Various Toxic Pollutants. *Int. J. Environ. Anal. Chem.* **2021**. [CrossRef]
60. Benettayeb, A.; Usman, M.; Tinashe, C.C.; Adam, T.; Haddou, B. A Critical Review with Emphasis on Recent Pieces of Evidence of *Moringa Oleifera* Biosorption in Water and Wastewater Treatment. *Environ. Sci. Pollut. Res.* **2022**, *29*, 48185–48209. [CrossRef] [PubMed]
61. Fosso-Kankeu, E.; Mulaba-Bafubiandi, A.F. Review of Challenges in the Escalation of Metal-Biosorbing Processes for Wastewater Treatment: Applied and Commercialized Technologies. *Afr. J. Biotechnol.* **2014**, *13*, 1756–1771. [CrossRef]
62. Górecka, E.; Jastrzębska, M. Review Article: Immobilization Techniques and Biopolymer Carriers. *Biotechnol. Food Sci.* **2011**, *75*, 65–86.
63. Wang, J.; Chen, C. Biosorbents for Heavy Metals Removal and Their Future. *Biotechnol. Adv.* **2009**, *27*, 195–226. [CrossRef]
64. de Freitas, G.R.; da Silva, M.G.C.; Vieira, M.G.A. Biosorption Technology for Removal of Toxic Metals: A Review of Commercial Biosorbents and Patents. *Environ. Sci. Pollut. Res.* **2019**, *26*, 19097–19118. [CrossRef]

65. Moghadas, B.K.; Esmaeili, H.; Tamjidi, S.; Geramifard, A. Advantages of Nanoadsorbents, Biosorbents, and Nanobiosorbents for Contaminant Removal. In *Nano-Biosorbents for Decontamination of Water, Air, and Soil Pollution*; Elsevier: Amsterdam, The Netherlands, 2022; pp. 105–133. [[CrossRef](#)]
66. Vagheti, J.C.P.; Lima, E.C.; Royer, B.; da Cunha, B.M.; Cardoso, N.F.; Brasil, J.L.; Dias, S.L.P. Pecan Nutshell as Biosorbent to Remove Cu(II), Mn(II) and Pb(II) from Aqueous Solutions. *J. Hazard. Mater.* **2009**, *162*, 270–280. [[CrossRef](#)] [[PubMed](#)]
67. Liu, C.; Ngo, H.H.; Guo, W. Watermelon Rind: Agro-Waste or Superior Biosorbent? *Appl. Biochem. Biotechnol.* **2012**, *167*, 1699–1715. [[CrossRef](#)] [[PubMed](#)]
68. Akunwa, N.K.; Muhammad, M.N.; Akunna, J.C. Treatment of Metal-Contaminated Wastewater: A Comparison of Low-Cost Biosorbents. *J. Environ. Manag.* **2014**, *146*, 517–523. [[CrossRef](#)] [[PubMed](#)]
69. Banerjee, K. A Novel Agricultural Waste Adsorbent, Watermelon Shell for the Removal of Copper from Aqueous Solutions. *Iran. J. Energy Environ.* **2012**, *3*, 143–156. [[CrossRef](#)]
70. Song, Y.; Jin, L.; Wang, X. Cadmium Absorption and Transportation Pathways in Plants. *Int. J. Phytoremediat.* **2017**, *19*, 133–141. [[CrossRef](#)]
71. Anastopoulos, I.; Pashalidis, I.; Hosseini-Bandegharai, A.; Giannakoudakis, D.A.; Robalds, A.; Usman, M.; Escudero, L.B.; Zhou, Y.; Colmenares, J.C.; Núñez-Delgado, A.; et al. Agricultural Biomass/Waste as Adsorbents for Toxic Metal Decontamination of Aqueous Solutions. *J. Mol. Liq.* **2019**, *295*, 111684. [[CrossRef](#)]
72. Wang, Q.; Wang, Y.; Yang, Z.; Han, W.; Yuan, L.; Zhang, L.; Huang, X. Efficient Removal of Pb(II) and Cd(II) from Aqueous Solutions by Mango Seed Biosorbent. *Chem. Eng. J. Adv.* **2022**, *11*, 100295. [[CrossRef](#)]
73. Wang, X.S.; Qin, Y.; Li, Z.F. Biosorption of Zinc from Aqueous Solutions by Rice Bran: Kinetics and Equilibrium Studies. *Sep. Sci. Technol.* **2006**, *41*, 747–756. [[CrossRef](#)]
74. Yin, K.; Wang, Q.; Lv, M.; Chen, L. Microorganism Remediation Strategies towards Heavy Metals. *Chem. Eng. J.* **2019**, *360*, 1553–1563. [[CrossRef](#)]
75. Marín-Rangel, V.M.; Cortés-Martínez, R.; Cuevas Villanueva, R.A.; Garnica-Romo, M.G.; Martínez-Flores, H.E. As (V) Biosorption in an Aqueous Solution Using Chemically Treated Lemon (*Citrus Aurantifolia* Swingle) Residues. *J. Food Sci.* **2012**, *77*, T10–T14. [[CrossRef](#)]
76. Nguyen, H.D.; Tran, H.N.; Chao, H.P.; Lin, C.C. Activated Carbons Derived from Teak Sawdust-Hydrochars for Efficient Removal of Methylene Blue, Copper, and Cadmium from Aqueous Solution. *Water* **2019**, *11*, 2581. [[CrossRef](#)]
77. Tarrés, Q.; Oliver-Ortega, H.; Boufi, S.; Àngels Pèlach, M.; Delgado-Aguilar, M.; Mutjé, P. Evaluation of the Fibrillation Method on Lignocellulosic Nanofibers Production from Eucalyptus Sawdust: A Comparative Study between High-Pressure Homogenization and Grinding. *Int. J. Biol. Macromol.* **2020**, *145*, 1199–1207. [[CrossRef](#)] [[PubMed](#)]
78. Parthasarathy, P.; Narayanan, K.S. Hydrogen Production from Steam Gasification of Biomass: Influence of Process Parameters on Hydrogen Yield—A Review. *Renew. Energy* **2014**, *66*, 570–579. [[CrossRef](#)]
79. Zhou, K.; Yang, Z.; Liu, Y.; Kong, X. Kinetics and Equilibrium Studies on Biosorption of Pb(II) from Aqueous Solution by a Novel Biosorbent: *Cyclosorus Interruptus*. *J. Environ. Chem. Eng.* **2015**, *3*, 2219–2228. [[CrossRef](#)]
80. Ashrafi, S.D.; Kamani, H.; Soheil Arezomand, H.; Yousefi, N.; Mahvi, A.H. Optimization and Modeling of Process Variables for Adsorption of Basic Blue 41 on NaOH-Modified Rice Husk Using Response Surface Methodology. *Desalination Water Treat.* **2015**, *57*, 14051–14059. [[CrossRef](#)]
81. Jung, B.; Farzaneh, H.; Khodary, A.; Abdel-Wahab, A. Photochemical Degradation of Trichloroethylene by Sulfite-Mediated UV Irradiation. *J. Environ. Chem. Eng.* **2015**, *3*, 2194–2202. [[CrossRef](#)]
82. Sud, D.; Mahajan, G.; Kaur, M.P. Agricultural Waste Material as Potential Adsorbent for Sequestering Heavy Metal Ions from Aqueous Solutions—A Review. *Bioresour. Technol.* **2008**, *99*, 6017–6027. [[CrossRef](#)]
83. Shafique, U.; Ijaz, A.; Salman, M.; Zaman, W.U.; Jamil, N.; Rehman, R.; Javaid, A. Removal of Arsenic from Water Using Pine Leaves. *J. Taiwan Inst. Chem. Eng.* **2012**, *43*, 256–263. [[CrossRef](#)]
84. Reddy, D.H.K.; Harinath, Y.; Seshiah, K.; Reddy, A.V.R. Biosorption of Pb(II) from Aqueous Solutions Using Chemically Modified *Moringa Oleifera* Tree Leaves. *Chem. Eng. J.* **2010**, *162*, 626–634. [[CrossRef](#)]
85. Doğan, M.; Abak, H.; Alkan, M. Adsorption of Methylene Blue onto Hazelnut Shell: Kinetics, Mechanism and Activation Parameters. *J. Hazard. Mater.* **2009**, *164*, 172–181. [[CrossRef](#)]
86. Guimarães Gusmão, K.A.; Alves Gurgel, L.V.; Sacramento Melo, T.M.; Gil, L.F. Application of Succinylated Sugarcane Bagasse as Adsorbent to Remove Methylene Blue and Gentian Violet from Aqueous Solutions—Kinetic and Equilibrium Studies. *Dye. Pigment.* **2012**, *92*, 967–974. [[CrossRef](#)]
87. Saha, P.; Chowdhury, S.; Gupta, S.; Kumar, I. Insight into Adsorption Equilibrium, Kinetics and Thermodynamics of Malachite Green onto Clayey Soil of Indian Origin. *Chem. Eng. J.* **2010**, *165*, 874–882. [[CrossRef](#)]
88. Chen, J.; Shi, X.; Zhan, Y.; Qiu, X.; Du, Y.; Deng, H. Construction of Horizontal Stratum Landform-like Composite Foams and Their Methyl Orange Adsorption Capacity. *Appl. Surf. Sci.* **2017**, *397*, 133–143. [[CrossRef](#)]
89. Ohs, B.; Krödel, M.; Wessling, M. Adsorption of Carbon Dioxide on Solid Amine-Functionalized Sorbents: A Dual Kinetic Model. *Sep. Purif. Technol.* **2018**, *204*, 13–20. [[CrossRef](#)]
90. Ahmed, S.M.; Taha, M.R.; Taha, O.M.E. Kinetics and Isotherms of Dichlorodiphenyltrichloroethane (DDT) Adsorption Using Soil–Zeolite Mixture. *Nanotechnol. Environ. Eng.* **2018**, *3*, 4. [[CrossRef](#)]

91. Baral, S.S.; Das, N.; Roy Chaudhury, G.; Das, S.N. A Preliminary Study on the Adsorptive Removal of Cr(VI) Using Seaweed, *Hydrilla verticillata*. *J. Hazard. Mater.* **2009**, *171*, 358–369. [CrossRef]
92. Oluwaseyi, A.A.; Solomon, O.A.; Abayomi, B.; Demilade, T.A.; Morenike, O.A.; Omolabake, A.O.A.; Tosin, A.A.; Adedamola, T.O.; Kayode, A.A.; Olugbenga, S.B. Adsorptive Removal of Antibiotic Pollutants from Wastewater Using Biomass/biochar-based Adsorbents. *RSC Adv.* **2023**, *13*, 4678. [CrossRef]
93. Kayode, A.A.; Oreoluwa, O.A.; Omolabake, A.O.A.; Oyeladun, R.A.; Abdullahi, B.O.; Oluwaseyi, A.A.; Halimat, O.; Nobanathi, W.M.; Olugbenga, S.B. Sawdust-biomass based Materials for Sequestration of Organic and Inorganic Pollutants and Potential for Engineering Applications. *Curr. Res. Green Sustain. Chem.* **2022**, *5*, 100274.
94. Shagufta, Z.; Muhammad, I.K.; Nouredine, E.; Mushtaq, H.L.; Abdallah, S.; Shabnam, S.; Suryyia, M. Adsorption Performance of Rice Husk towards Copper Ions from Wastewater. *Desalination Water Treat.* **2022**, *258*, 133–142.
95. Huang, Y.-D.-D. Comments on Using of “Pseudo-First-Order Model” [Appl. Surf. Sci. 394 (2017) 378–385, 397 (2017) 133–143, 426 (2017) 545–553, 437 (2018) 294–303]. *Appl. Surf. Sci.* **2019**, *469*, 564–565. [CrossRef]
96. Afroze, S.; Sen, T.K. A Review on Heavy Metal Ions and Dye Adsorption from Water by Agricultural Solid Waste Adsorbents. *Water Air Soil Pollut.* **2018**, *229*, 1–50. [CrossRef]
97. Chowdhury, S.; Saha, P. Sea Shell Powder as a New Adsorbent to Remove Basic Green 4 (Malachite Green) from Aqueous Solutions: Equilibrium, Kinetic and Thermodynamic Studies. *Chem. Eng. J.* **2010**, *164*, 168–177. [CrossRef]
98. Yao, Z.Y.; Qi, J.H.; Wang, L.H. Equilibrium, Kinetic and Thermodynamic Studies on the Biosorption of Cu(II) onto Chestnut Shell. *J. Hazard. Mater.* **2010**, *174*, 137–143. [CrossRef]
99. Weber, W.J.; Morris, J.C. Kinetics of Adsorption on Carbon from Solution. *J. Sanit. Eng. Div.* **1963**, *89*, 31–59. [CrossRef]
100. Wang, K.; Ren, H.; Wang, Z.; Ma, S.; Wei, J.; Ke, W.; Guo, Y. Kinetic Characteristics of CH₄ Adsorption on Coals under Variable Temperature–Pressure Coupling Interaction. *Nat. Resour. Res.* **2021**, *30*, 4597–4620. [CrossRef]
101. Aharoni, C.; Ungarish, M. Kinetics of Activated Chemisorption. Part 2.—Theoretical Models. *J. Chem. Soc. Faraday Trans. 1: Phys. Chem. Condens. Phases* **1977**, *73*, 456–464. [CrossRef]
102. Zhou, J.; Zhang, C.; Du, B.; Cui, H.; Fan, X.; Zhou, D.; Zhou, J. Effects of Zinc Application on Cadmium (Cd) Accumulation and Plant Growth through Modulation of the Antioxidant System and Translocation of Cd in Low- and High-Cd Wheat Cultivars. *Environ. Pollut.* **2020**, *265*, 115045. [CrossRef]
103. Zhou, Q.; Gao, Q.; Luo, W.; Yan, C.; Ji, Z.; Duan, P. One-Step Synthesis of Amino-Functionalized Attapulgite Clay Nanoparticles Adsorbent by Hydrothermal Carbonization of Chitosan for Removal of Methylene Blue from Wastewater. *Colloids Surf. A Physicochem. Eng. Asp.* **2015**, *470*, 248–257. [CrossRef]
104. Zhou, C.; Wu, Q.; Lei, T.; Negulescu, I.I. Adsorption Kinetic and Equilibrium Studies for Methylene Blue Dye by Partially Hydrolyzed Polyacrylamide/Cellulose Nanocrystal Nanocomposite Hydrogels. *Chem. Eng. J.* **2014**, *251*, 17–24. [CrossRef]
105. Zhou, L.; Xu, X.; Xia, S. Effects of Sulfate on Simultaneous Nitrate and Selenate Removal in a Hydrogen-Based Membrane Biofilm Reactor for Groundwater Treatment: Performance and Biofilm Microbial Ecology. *Chemosphere* **2018**, *211*, 254–260. [CrossRef]
106. Langmuir, I. The Constitution and Fundamental Properties of Solids and Liquids. *J. Am. Chem. Soc.* **1916**, *38*, 2221–2295. [CrossRef]
107. Freundlich, H.M.F. Over the Adsorption in Solution. *J. Phys. Chem.* **1906**, *57*, 385–471.
108. Bohart, G.S.; Adams, E.Q. Some Aspects of the Behavior of Charcoal with Respect to Chlorine. *J. Am. Chem. Soc.* **1920**, *42*, 523–544. [CrossRef]
109. Bruanuer, S.; Emmett, P.H.; Teller, E. Adsorption of Gases in Multimolecular Layers. *J. Am. Chem. Soc.* **1938**, *60*, 309–316. [CrossRef]
110. Dubinin, M.M.; Radushkevich, L.V. The Equation of the Characteristic Curve of the Activated Charcoal. *Proc. Acad. Sci. USSR Phys. Chem. Sect.* **1947**, *55*, 331–337.
111. Saadi, R.; Saadi, Z.; Fazaeli, R.; Fard, N.E. Monolayer and Multilayer Adsorption Isotherm Models for Sorption from Aqueous Media. *Korean J. Chem. Eng.* **2015**, *32*, 787–799. [CrossRef]
112. Hill, T.L. Theory of Physical Adsorption. *Adv. Catal.* **1952**, *4*, 211–258.
113. Khan, A.R.; Ataullah, R.; Al-Haddad, A. Equilibrium Adsorption Studies of Some Aromatic Pollutants from Dilute Aqueous Solutions on Activated Carbon at Different Temperatures—ScienceDirect. Available online: <https://www.sciencedirect.com/science/article/abs/pii/S0021979797950414> (accessed on 23 May 2022).
114. Koble, R.A.; Corrigan, T.E. Adsorption Isotherms for Pure Hydrocarbons. *Ind. Eng. Chem.* **1952**, *44*, 383–387. [CrossRef]
115. McMillan, W.G.; Teller, E. The Assumptions of the B.E.T. Theory. *J. Phys. Colloid Chem.* **1951**, *55*, 17–20. [CrossRef] [PubMed]
116. Myers, A.L.; Prausnitz, J.M. Thermodynamics of Mixed-Gas Adsorption. *AIChE J.* **1965**, *11*, 121–127. [CrossRef]
117. Redlich, O.; Peterson, D.L. A Useful Adsorption Isotherm. *J. Phys. Chem.* **1959**, *63*, 1024. [CrossRef]
118. Sips, R. Combined Form of Langmuir and Freundlich Equations. *J. Chem. Phys.* **1948**, *16*, 490–495. [CrossRef]
119. Tempkin, M.I.; Pyzhev, V. Kinetics of Ammonia Synthesis on Promoted Iron Catalyst. *Acta Phys. Chim.* **1940**, *12*, 327–356.
120. Toth, J. State Equations of the Solid Gas Interface Layer. *Acta Chem. Acad. Hung.* **1971**, *69*, 311–317.
121. Das, S.; Barui, A.; Adak, A. Montmorillonite Impregnated Electrospun Cellulose Acetate Nanofiber Sorptive Membrane for Ciprofloxacin Removal from Wastewater. *J. Water Process. Eng.* **2020**, *37*, 101497. [CrossRef]
122. Ahmed, M.J.; Hameed, B.H. Removal of Emerging Pharmaceutical Contaminants by Adsorption in a Fixed-Bed Column: A Review. *Ecotoxicol. Environ. Saf.* **2018**, *149*, 257–266. [CrossRef]

123. Wahab, M.; Zahoor, M.; Muhammad Salman, S.; Kamran, A.W.; Naz, S.; Burlakovs, J.; Zekker, I. Adsorption-Membrane Hybrid Approach for the Removal of Azithromycin from Water: An Attempt to Minimize Drug Resistance Problem. *Water* **2021**, *13*, 1969. [CrossRef]
124. Elovich, S.Y.; Larionov, O.G. Theory of Adsorption from 11, Nonelectrolyte Solutions on Solid Adsorbents. *Russ. Chem. Bull.* **1962**, *11*, 198–203. [CrossRef]
125. Zhou, Y.; Liu, X.; Tang, L.; Zhang, F.; Zeng, G.; Peng, X.; Luo, L.; Deng, Y.; Pang, Y.; Zhang, J. Insight into Highly Efficient Co-Removal of p-Nitrophenol and Lead by Nitrogen-Functionalized Magnetic Ordered Mesoporous Carbon: Performance and Modelling. *J. Hazard. Mater.* **2017**, *333*, 80–87. [CrossRef] [PubMed]
126. Bertoldi, D.; Villegas, T.R.; Larcher, R.; Santato, A.; Nicolini, G. Arsenic Present in the Soil-Vine-Wine Chain in Vineyards Situated in an Old Mining Area in Trentino, Italy. *Environ. Toxicol. Chem.* **2013**, *32*, 773–779. [CrossRef]
127. Kutluay, S. Excellent Adsorptive Performance of Novel Magnetic Nano-Adsorbent Functionalized with 8-Hydroxyquinoline-5-Sulfonic Acid for the Removal of Volatile Organic Compounds (BTX) Vapors. *Fuel* **2021**, *287*, 119691. [CrossRef]
128. Oluwatobi, S.A.; Olugbenga, S.B. Enhanced Adsorption of Ciprofloxacin from Aqueous Solutions Using Functionalized Banana Stalk. *Biomass Convers. Biorefin.* **2020**, *12*, 5463–5478. [CrossRef]
129. Jin, C.; Sun, J.; Chen, Y.; Guo, Y.; Han, D.; Wang, R.; Zhao, C. Sawdust Wastes-Derived Porous Carbons for CO₂ Adsorption. Part 1. Optimization Preparation via Orthogonal Experiment. *Sep. Purif. Technol.* **2021**, *276*, 119270. [CrossRef]
130. Yu, Z.; Zhou, L.; Huang, Y.; Song, Z.; Qiu, W. Effects of a Manganese Oxide-Modified Biochar Composite on Adsorption of Arsenic in Red Soil. *J. Environ. Manag.* **2015**, *163*, 155–162. [CrossRef] [PubMed]
131. Jiang, L.; Liu, Y.; Zeng, G.; Liu, S.; Hu, X.; Zhou, L.; Tan, X.; Liu, N.; Li, M.; Wen, J. Adsorption of Estrogen Contaminants (17 β -Estradiol and 17 α -Ethinylestradiol) by Graphene Nanosheets from Water: Effects of Graphene Characteristics and Solution Chemistry. *Chem. Eng. J.* **2018**, *339*, 296–302. [CrossRef]
132. Tuomikoski, S.; Runtti, H.; Romar, H.; Lassi, U.; Kangas, T. Multiple Heavy Metal Removal Simultaneously by a Biomass-Based Porous Carbon. *Water Environ. Res.* **2021**, *93*, 1303–1314. [CrossRef]
133. Alabarse, F.G.; Conceição, R.V.; Balzaretto, N.M.; Schenato, F.; Xavier, A.M. In-Situ FTIR Analyses of Bentonite under High-Pressure. *Appl. Clay Sci.* **2011**, *51*, 202–208. [CrossRef]
134. Flory, P.J. Thermodynamics of Crystallization in High Polymers. I. Crystallization Induced by Stretching. *J. Chem. Phys.* **1947**, *15*, 397–408. [CrossRef]
135. Foo, K.Y.; Hameed, B.H. Mesoporous Activated Carbon from Wood Sawdust by K₂CO₃ Activation Using Microwave Heating. *Bioresour. Technol.* **2012**, *111*, 425–432. [CrossRef]
136. Njoku, V.O.; Foo, K.Y.; Asif, M.; Hameed, B.H. Preparation of Activated Carbons from Rambutan (*Nephelium Lappaceum*) Peel by Microwave-Induced KOH Activation for Acid Yellow 17 Dye Adsorption. *Chem. Eng. J.* **2014**, *250*, 198–204. [CrossRef]
137. Foo, K.Y.; Hameed, B.H. Preparation and Characterization of Activated Carbon from Pistachio Nut Shells via Microwave-Induced Chemical Activation. *Biomass Bioenergy* **2011**, *35*, 3257–3261. [CrossRef]
138. Inyang, M.I.; Gao, B.; Yao, Y.; Xue, Y.; Zimmerman, A.; Mosa, A.; Pullammanappallil, P.; Ok, Y.S.; Cao, X. A Review of Biochar as a Low-Cost Adsorbent for Aqueous Heavy Metal Removal. *Crit. Rev. Environ. Sci. Technol.* **2016**, *46*, 406–433. [CrossRef]
139. Yu, J.; Tang, T.; Cheng, F.; Huang, D.; Martin, J.L.; Brewer, C.E.; Grimm, R.L.; Zhou, M.; Luo, H. Waste-to-Wealth Application of Wastewater Treatment Algae-Derived Hydrochar for Pb(II) Adsorption. *MethodsX* **2021**, *8*, 101263. [CrossRef]
140. Doebele, V. Condensation et Évaporation de l'Hexane Dans Les Membranes d'Alumine Poreuse (Condensation and Evaporation of Hexane). Ph.D. Thesis, Université Grenoble Alpes (ComUE), Saint-Martin-d'Hères, France, 2019. Available online: <https://www.theses.fr/2019GREAY021> (accessed on 17 March 2023).
141. Kayode, M.O.; Victor, A.J.; Oluwaseun, F.G.; Opeyemi, O.O.; Samuel, O.A.; Kudirat, J.L. Biosorption Potentials of Sawdust in Removing Zinc Ions from Aqueous Solution. *Int. J. Sci. Res. Manag. (IJSRM)* **2021**, *9*, FE-2021-191-198.
142. Tran, H.N.; Lima, E.C.; Juang, R.S.; Bollinger, J.C.; Chao, H.P. Thermodynamic Parameters of Liquid-Phase Adsorption Process Calculated from Different Equilibrium Constants Related to Adsorption Isotherms: A Comparison Study. *J. Environ. Chem. Eng.* **2021**, *9*, 106674. [CrossRef]
143. Wang, S.; Kwak, J.H.; Islam, M.S.; Naeth, M.A.; Gamal El-Din, M.; Chang, S.X. Biochar Surface Complexation and Ni(II), Cu(II), and Cd(II) Adsorption in Aqueous Solutions Depend on Feedstock Type. *Sci. Total. Environ.* **2020**, *712*, 136538. [CrossRef] [PubMed]
144. Nwakonobi, T.U.; Onoja, S.B.; Ogbaje, H. Removal of Certain Heavy Metals from Brewery Wastewater Using Date Palm Seeds Activated Carbon. *Appl. Eng. Agric.* **2018**, *34*, 233–238. [CrossRef]
145. Crini, G.; Lichtfouse, E.; Wilson, L.; Morin-crini, N.; Crini, G.; Lichtfouse, E.; Wilson, L.; Conventional, N.M. *Conventional and Non-Conventional Adsorbents for Wastewater Treatment (Hal-02082916 Conventional and Non-Conventional Adsorbents for Wastewater Treatment)*; Springer: Cham, Switzerland, 2019; Volume 17, ISBN 9783319921112.
146. Singh, S.R.; Singh, A.P. Adsorption of Heavy Metals from Waste Waters Using Waste Biomass. *Int. J. Eng. Res.* **2017**, *V6*, 423–428. [CrossRef]
147. Singh, J.; Mishra, V. Simultaneous Removal of Cu²⁺, Ni²⁺ and Zn²⁺ Ions Using Leftover Azadirachta Indica Twig Ash. *Bioremediat. J.* **2020**, *25*, 48–71. [CrossRef]
148. Obeng, G.Y.; Amoah, D.Y.; Opoku, R.; Sekyere, C.K.K.; Adjei, E.A.; Mensah, E. Coconut Wastes as Bioresource for Sustainable Energy: Quantifying Wastes, Calorific Values and Emissions in Ghana. *Energies* **2020**, *13*, 2178. [CrossRef]

149. Wang, B.; Jiang, Y.S.; Li, F.Y.; Yang, D.Y. Preparation of Biochar by Simultaneous Carbonization, Magnetization and Activation for Norfloxacin Removal in Water. *Bioresour. Technol.* **2017**, *233*, 159–165. [[CrossRef](#)]
150. Szewczuk-Karpisz, K.; Wiśniewska, M.; Medykowska, M.; Galaburda, M.V.; Bogatyrov, V.M.; Oranska, O.I.; Błachnio, M.; Oleszczuk, P. Simultaneous Adsorption of Cu(II) Ions and Poly(Acrylic Acid) on the Hybrid Carbon-Mineral Nanocomposites with Metallic Elements. *J. Hazard. Mater.* **2021**, *412*, 125138. [[CrossRef](#)] [[PubMed](#)]
151. Vidyasagar, S.; Nesrin, O.; Martin, O.; Lars, B.; Stefan, K.; Robert, L. Thermogravimetric Analysis of Activated Carbons, Ordered Mesoporous Carbide-Derived Carbons, and Their Deactivation Kinetics of Catalytic Methane Decomposition. *Ind. Eng. Chem. Res.* **2014**, *53*, 1741–1753. [[CrossRef](#)]
152. Chieng, H.I.; Lim, L.B.L.; Priyantha, N. Enhancing Adsorption Capacity of Toxic Malachite Green Dye through Chemically Modified Breadnut Peel: Equilibrium, Thermodynamics, Kinetics and Regeneration Studies. *Environ. Technol.* **2015**, *36*, 86–97. [[CrossRef](#)] [[PubMed](#)]
153. Sips, R. On the Structure of a Catalyst Surface. *J. Chem. Phys.* **1948**, *16*, 490–495. [[CrossRef](#)]
154. Essandoh, M.; Kunwar, B.; Pittman, C.U.; Mohan, D.; Mlsna, T. Sorptive Removal of Salicylic Acid and Ibuprofen from Aqueous Solutions Using Pine Wood Fast Pyrolysis Biochar. *Chem. Eng. J.* **2015**, *265*, 219–227. [[CrossRef](#)]
155. Foo, K.Y.; Hameed, B.H. Insights into the Modeling of Adsorption Isotherm Systems. *Chem. Eng. J.* **2010**, *156*(1), 2–10. [[CrossRef](#)]
156. Olugbenga, S.B.; Esther, O.A.; Kayode, A.A.; Samuel, A.A.; Adejumoke, A.I.; Adewumi, O.D. Rhodamine B Dye Sequestration Using Gmelina Aborea Leaf Powder. *Heliyon* **2019**, *5*, e02872. [[CrossRef](#)]
157. Zare, E.N.; Motahari, A.; Sillanpää, M. Nano-adsorbents Based on Conducting Polymer Nanocomposites with Main Focus on Polyaniline and Its Derivatives for Removal of Heavy Metal Ions/Dyes: A Review. *Environ. Res.* **2018**, *162*, 173–195. [[CrossRef](#)]
158. Rosa, L.M.T.; Botero, W.G.; do Carmo, J.B.; Gabriel, G.V.M.; Waldman, W.R.; Cavagis, A.D.M.; Goveia, D.; de Oliveira, L.C. Application of Natural Organic Residues in the Remediation of Metals from E-Waste. *Environ. Technol. Innov.* **2022**, *27*, 102452. [[CrossRef](#)]
159. Ali, I.; Peng, C.; Naz, I. Removal of Lead and Cadmium Ions by Single and Binary Systems Using Phytogenic Magnetic Nanoparticles Functionalized by 3-Mercaptopropanoic Acid. *Chin. J. Chem. Eng.* **2019**, *27*, 949–964. [[CrossRef](#)]
160. Al-Ghouti, M.A.; Da'ana, D.A. Guidelines for the Use and Interpretation of Adsorption Isotherm Models: A Review. *J. Hazard. Mater.* **2020**, *393*, 122383. [[CrossRef](#)] [[PubMed](#)]
161. Wu, Z.; Chen, X.; Yuan, B.; Fu, M.L. A Facile Foaming-Polymerization Strategy to Prepare 3D MnO₂ Modified Biochar-Based Porous Hydrogels for Efficient Removal of Cd(II) and Pb(II). *Chemosphere* **2020**, *239*, 124745. [[CrossRef](#)] [[PubMed](#)]
162. Zhou, X.; Zhou, J.; Liu, Y.; Guo, J.; Ren, J.; Zhou, F. Preparation of Iminodiacetic Acid-Modified Magnetic Biochar by Carbonization, Magnetization and Functional Modification for Cd(II) Removal in Water. *Fuel* **2018**, *233*, 469–479. [[CrossRef](#)]

Disclaimer/Publisher's Note: The statements, opinions and data contained in all publications are solely those of the individual author(s) and contributor(s) and not of MDPI and/or the editor(s). MDPI and/or the editor(s) disclaim responsibility for any injury to people or property resulting from any ideas, methods, instructions or products referred to in the content.